

AD-A059 636

HONEYWELL INC HOPKINS MINN
MINI-REFRACTION SONDE FIELD TESTS.(U)
DEC 77 C D MOTCHENBACHER

F/G 4/2

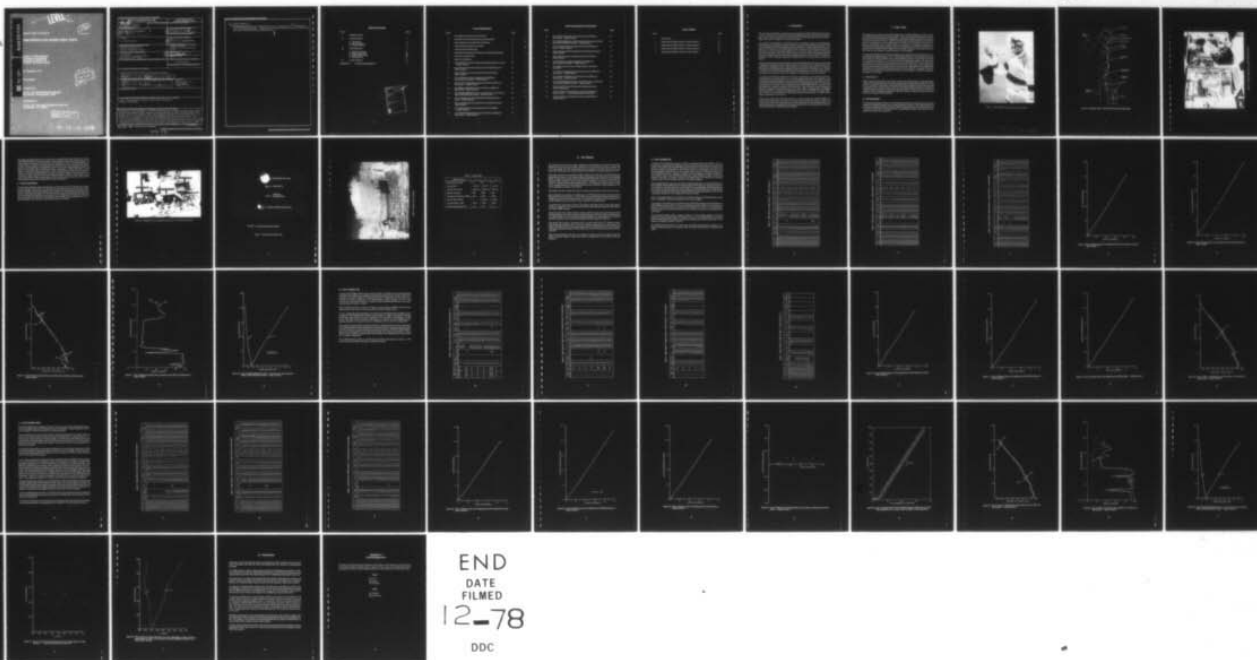
N62269-76-C-0368

UNCLASSIFIED

NADC-76128-30-B

NL

| OF |
AD
A059636



END
DATE
FILMED
12-78
DDC

AD A059636

DDC FILE COPY

AD57416
LEVEL
86
(12)
Report NADC-76128-30-B ✓

MINI-REFRACTION SONDE FIELD TESTS

Curtis D. Motchenbacher
Honeywell Incorporated
600 Second Street N.E.
Hopkins, Minnesota 55343

30 December 1977

Final Report

Prepared for

NAVAL AIR DEVELOPMENT CENTER
Warminster, Pennsylvania 18974

Sponsored by

NAVAL AIR SYSTEMS COMMAND (AIR-370)
Washington, D.C. 20631

DDC
OCT 11 1978
F

This document has been approved
for public release and sale; its
distribution is unlimited.

78 10 05 058

SECURITY CLASSIFICATION OF THIS PAGE (WHEN DATA ENTERED)

REPORT DOCUMENTATION PAGE		READ INSTRUCTIONS BEFORE COMPLETING FORM
1. REPORT NUMBER NADC-76128-30-B	2. GOV'T ACCESSION NUMBER	3. RECIPIENT'S CATALOG NUMBER
4. TITLE (AND SUBTITLE) MINI-REFRACTION SONDE FIELD TESTS	5. TYPE OF REPORT/PERIOD COVERED Final Summary Report	
7. AUTHOR(S) C. Motchenbacher	6. PERFORMING ORG. REPORT NUMBER	
9. PERFORMING ORGANIZATION NAME/ADDRESS Honeywell Incorporated 600 Second Street, N. E. Hopkins, Minnesota 55343	8. CONTRACT OR GRANT NUMBER(S) N62269-76-C-0368/P00002	
11. CONTROLLING OFFICE NAME/ADDRESS Commander Naval Air Development Center Warminster, Pa. 18974	10. PROGRAM ELEMENT, PROJECT, TASK AREA & WORK UNIT NUMBERS 62759N F52-551 WF52551734 RG701	
14. MONITORING AGENCY NAME/ADDRESS (IF DIFFERENT FROM CONT. OFF.)	12. REPORT DATE 30 December 1977	
	13. NUMBER OF PAGES 53	
	15. SECURITY CLASSIFICATION (OF THIS REPORT) UNCLASSIFIED	
	15a. DECLASSIFICATION DOWNGRADING SCHEDULE	

16. DISTRIBUTION STATEMENT (OF THIS REPORT)

Approved for Public Release; Distribution Unlimited.

17. DISTRIBUTION STATEMENT (OF THE ABSTRACT ENTERED IN BLOCK 20, IF DIFFERENT FROM REPORT)

18. SUPPLEMENTARY NOTES

19. KEY WORDS (CONTINUE ON REVERSE SIDE IF NECESSARY AND IDENTIFY BY BLOCK NUMBER)

Sonde, Meteorological, Balloon, Barometer, Hygristor,
Battery Transmitter

20. ABSTRACT (CONTINUE ON REVERSE SIDE IF NECESSARY AND IDENTIFY BY BLOCK NUMBER)

The purpose of this program is to demonstrate that it is feasible to build a small, light-weight meteorological sonde capable of measuring index of refraction (Mini-Refracton Sonde), which can be launched with a 30-gram Pibal balloon. This minisonde uses a rod thermistor for temperature and a carbon hygistor for humidity measurement. For pressure measurement, a Honeywell silicon diaphragm barometer was used. This sensor uses a silicon diaphragm on an evacuated chamber with strain-sensitive resistor sensing. The sensors are electronically time-commutated on a 400-millisecond cycle. A light-weight telemetry transmitter provides 1/2 watt at 400 megahertz. Power is from a

(continued)

20. lithium battery.

Laboratory measurements demonstrate an rms accuracy of 0.5°C temperature and 0.8 millibar pressure. Flight tests show good operation and good agreement with radar and Rawinsonde measurements.

Table of Contents

Section	Page
I. INTRODUCTION	1
II. FLIGHT TESTS	2
A. Test Facility	2
B. Test Equipment	2
C. Flight Conditions	8
III. TEST RESULTS	13
A. Flight Number One	14
B. Flight Number Two	25
C. Flight Number Three	36
D. Data Reduction	49
IV. CONCLUSIONS	52
APPENDIX A ACKNOWLEDGEMENTS	53

ACCESSION for	
NTIS	White Section <input checked="" type="checkbox"/>
DDC	Buff Section <input type="checkbox"/>
UNANNOUNCED <input type="checkbox"/>	
JUSTIFICATION	
BY	
DISTRIBUTION/AVAILABILITY NOTES	
Dist	
<div style="font-size: 2em; font-weight: bold; position: absolute; left: 10px; bottom: 10px;">A</div>	

List of Illustrations

Figure		Page
1	Mini-Refraction Sonde Used in Field Tests	3
2	Exploded View of Minisonde Showing Subassemblies	4
3	Support Equipment at NASA Met-Ops Facility	5
4	Meteorological Data Reduction Facility	6
5	Telemetry Antenna Mounting	7
6	Honeywell Ground Support Equipment in the Met-Ops Building	9
7	Sonde Launch Flight Train	10
8	Radar Corner Reflector	11
9	Plot of Altitude versus Time Measured with Mini-Refraction Sonde — Flight Number 1	18
10	Plot of Altitude versus Time Measured with NWS Rawinsonde — Flight Number 1	19
11	Plot of Altitude versus Time Measured with NASA Radar — Flight Number 1	20
12	Plot of Difference in Altitude Reading of the MRS and Rawinsonde versus Radar — Flight Number 1	21
13	Plot of Free-Air Temperature versus Altitude for the MRS and Rawinsonde — Flight Number 1	22
14	Plot of Relative Humidity versus Altitude for the MRS and Rawinsonde — Flight Number 1	23
15	Plot of Modified Refractive Index, N, and M-Units versus Altitude Read by Mini-Refraction Sonde — Flight Number 1	24
16	Plot of Altitude versus Time Measured with Mini-Refraction Sonde — Flight Number 2	30
17	Plot of Altitude versus Time Measured with NWS Rawinsonde — Flight Number 2	31
18	Plot of Altitude versus Time Measured with NASA Radar — Flight Number 2	32
19	Plot of Free-Air Temperature versus Altitude for the MRS and Rawinsonde — Flight Number 2	33

List of Illustrations (Concluded)

Figure		Page
20	Plot of Relative Humidity versus Altitude for the MRS and Rawinsonde — Flight Number 2	34
21	Plot of Modified Refractive Index, N, and M-Units versus Altitude Read by Mini-Refraction Sonde — Flight Number 2	35
22	Plot of Altitude versus Time Measured with Mini-Refraction Sonde — Flight Number 3	40
23	Plot of Altitude versus Time Measured with NWS Rawinsonde — Flight Number 3	41
24	Plot of Altitude versus Time Measured with NASA Radar — Flight Number 3	42
25	Plot of Difference in Altitude Reading of the MRS and Rawinsonde versus Radar — Flight Number 3	43
26	Plot of Altitude versus Time for Flight Number 3 Measured with MRS	44
27	Plot of Free-Air Temperature versus Altitude for the MRS and Rawinsonde — Flight Number 3	45
28	Plot of Relative Humidity versus Altitude for the MRS and Rawinsonde — Flight Number 3	46
29	Plot of Modified Refractive Index, N, and M-Units versus Altitude Read by Mini-Refraction Sonde — Flight Number 3	47
30	Plot of N and M versus Altitude with an Expanded Scale to Illustrate Resolution	48
31	Plot of N and M versus Altitude for the First 1000 Meters of Flight Number 1 — Data Plotted at Switch Points Only	50
32	Plot of N and M versus Altitude for the First 1000 Meters of Flight Number 1	51

List of Tables

Table		Page
1	Launch Data	12
2	Flight Data for Flight Number 1, Sonde Number 11	15
3	Flight Data for Flight Number 2, Sonde Number 10	26
4	Flight Data for Flight Number 2, Sonde Number 10	29
5	Flight Data for Flight Number 3, Sonde Number 9	37

I. Introduction

The Navy has a requirement to measure the vertical profile of index of refraction from sea level to above 15,000 feet. It is necessary to make these measurements from many sizes and classes of ships. Further, these measurements must be made under typical operating conditions of calm or high winds and from stopped to full operational speed.

The purpose of this program is to demonstrate that it is feasible to build a small, lightweight meteorological sonde capable of measuring index of refraction (Mini-Refraction Sonde), which can be launched with a 30-inch diameter, 30-gram pibal balloon. In many field applications, it is difficult to fill and launch a very large balloon, either because of space limitations or because of high winds or other environmental conditions. It is very useful to have a balloon no larger than 30 inches in diameter so that it can be filled within a room and carried out through a standard ship's door for launching. Tests show that a 30-gram latex balloon, when inflated to 30 inches in diameter, will lift a 100-gram minisonde, including battery, at an ascent rate of 800 feet per minute.

During the previous section of this program, it was demonstrated that a 100-gram sonde capable of measuring temperature, pressure and humidity, could be built. This minisonde used a rod thermistor for temperature and a carbon hygistor for humidity measurement. For pressure measurement, a Honeywell silicon diaphragm barometer was used. This pressure sensor consists of a small silicon chip with strain-sensitive resistors diffused into the surface. This sensor is mounted on an evacuated tube so that changes in absolute pressure can be measured.

To commutate between the temperature, pressure, and humidity sensors and encode the meteorological data measurements, a set of meteorological electronics was developed using commercially available integrated circuits. By use of integrated circuits, it is possible to achieve all the commutation functions in a small and particularly lightweight package. The sensors are commutated on a time basis, with a complete cycle every 400 milliseconds. At a rise rate of 1000 feet per minute, this gives a complete set of data every 7 feet of altitude. A special lightweight telemetry transmitter, providing an output of 1/2 watt at 400 to 406 megahertz, was designed and constructed by the Honeywell Defense Electronics Division (DEL-D), Annapolis, Maryland. Power for the transmitter and minisonde electronics was provided by a small lithium battery consisting of 5-1/2 A cells.

The purpose of this phase of the development is to conduct flight tests of the Mini-Refraction Sonde. Three sondes were launched at the NASA facility at Wallops Island, Virginia, and tracked with radar. The sondes operated well and telemetered the meteorological data to the ground. Minisonde data agreed well with the radar height and with measurements of the National Weather Service (NWS) Rawinsonde flight.

II. Flight Tests

The purpose of this contract was to perform flight tests on the Mini-Refraction Sonde. A photo of the Mini-Refraction Sonde is shown in Figure 1. The sonde is small and weighs less than 100 grams with the batteries installed. Temperature, humidity and pressure sensors are mounted in the upper section, while the meteorological electronics, battery and transmitter are in the lower section. An exploded view of the sonde is shown in Figure 2. A rod thermistor is used for temperature measurement and a carbon hygistor for humidity. For pressure measurement, a Honeywell silicon diaphragm barometer is used. This pressure sensor consists of a small silicon chip with strain-sensitive resistors diffused into the surface. This sensor is mounted on an evacuated tube so that changes in absolute pressure can be measured.

To commute between the temperature, pressure, and humidity sensors and encode the meteorological data measurements, a set of meteorological electronics was developed by using commercially available integrated circuits. With integrated circuits, it is possible to achieve all the commutation functions in a small and particularly lightweight package. The sensors are commutated on a time basis, with a complete cycle every 400 milliseconds. At a rise rate of 1000 feet per minute, this gives a complete set of data every 7 feet of altitude. A special, lightweight telemetry transmitter providing an output of 1/2 watt at 400 to 406 megahertz was designed and constructed by the Honeywell Defense Electronics Division (DEL-D), Annapolis, Maryland. Power for the transmitter and minisonde electronics was provided by a small lithium battery consisting of five A cells.

A. TEST FACILITY

Flight tests were performed at the NASA launch and tracking facility at Wallops Island, Virginia. Mini-Refraction Sonde launches were performed at the Met-Ops Building. The NASA facility is excellent for flight tests. It provides balloon filling, handling and launching, has radar to track the balloon train and read out altitude, and there are GMD antennas for tracking the 1680-MHz sonde. In addition, skilled personnel are available to give advice on launching and tracking. Some of the support equipment at Met-Ops is shown in Figure 3. Figure 4 shows the facility for reducing NWS sonde data.

B. TEST EQUIPMENT

Ground station equipment was set up in the Met-Ops building. The ground station receives and records the telemetered signals from the Mini-Refraction Sonde. A UHF corner reflector antenna was mounted on the roof as shown in Figure 5. Since the antenna is broadly directional, it is aimed in the direction of the sonde flight. A preamplifier was used at the antenna to compensate for losses on the long cable.



Figure 1. Mini-Refracton Sonde Used in Field Tests

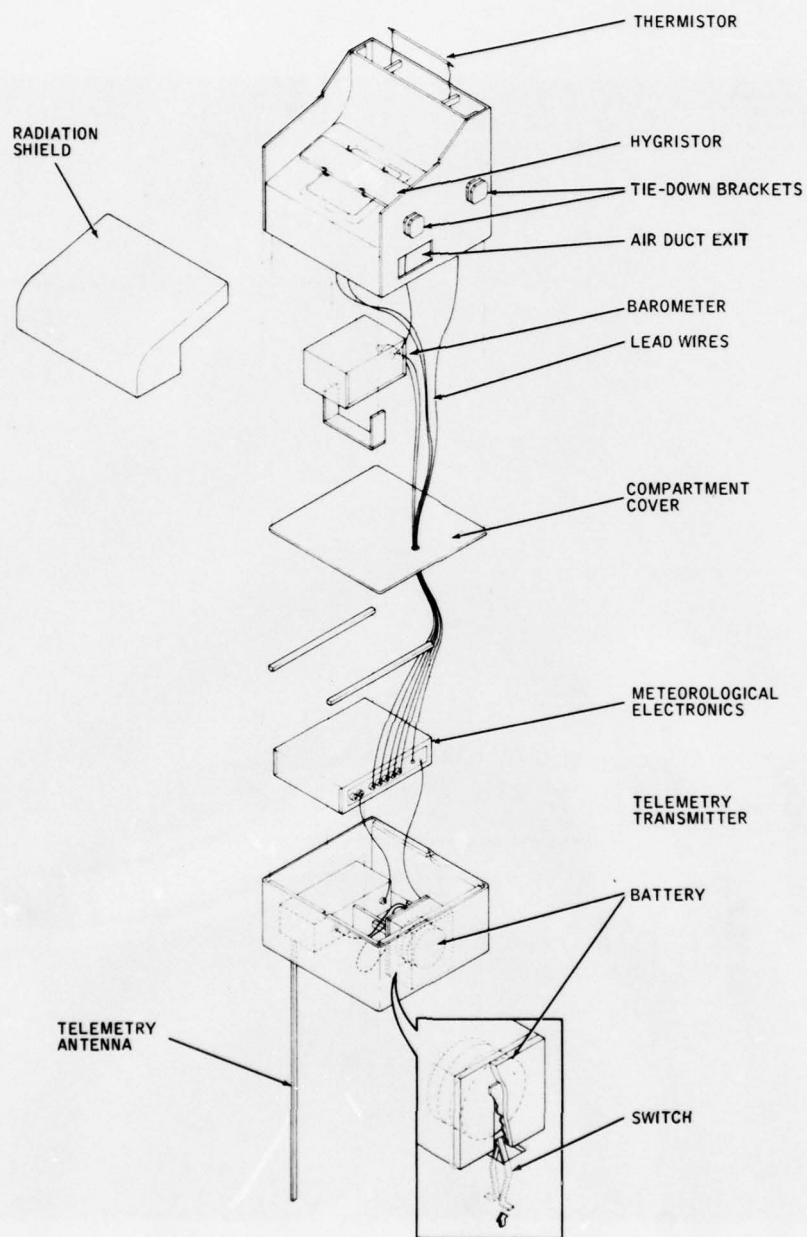


Figure 2. Exploded View of Minisonde Showing Subassemblies



Figure 3. Support Equipment at NASA Met-Ops Facility



Figure 4. Meteorological Data Reduction Facility

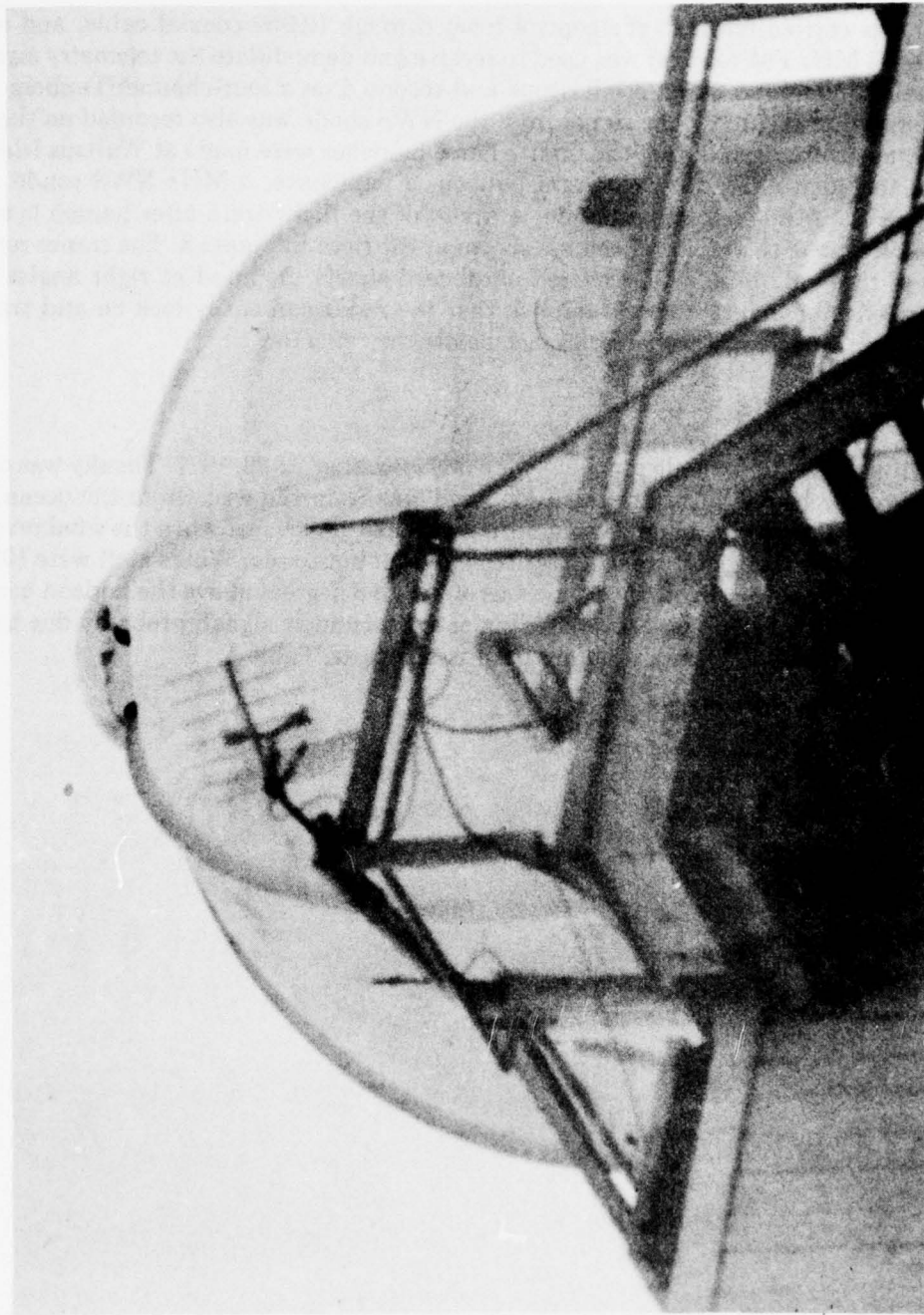


Figure 5. Telemetry Antenna Mounting

The signal was carried down to the control room through RG/59 coaxial cable, and a Nems-Clarke 400-406 MHz FM receiver was used to receive and demodulate the telemetry signal. The sonde signal is monitored on an oscilloscope and recorded on a four-channel Tanberg tape recorder, as shown in Figure 6. The signal from the NWS sonde was also recorded on the tape to provide a time comparison during the flight. Three launches were made at Wallops Island. The flight train included a 600- to 2000-gram balloon, a parachute, a MHz NWS sonde, a radar reflector, and the Mini-Refraction Sonde. A photo of the flight train after launch is shown in Figure 7. A closeup of the radar reflector is shown at the right in Figure 8. The corner reflector is composed of three aluminum foil-covered cardboard sheets mounted at right angles to each other. This reflector makes a good target so that the radar can easily lock on and track. The Mini-Refraction Sonde was tethered 25 feet below the reflector.

C. FLIGHT CONDITIONS

The three Mini-Refraction Sonde launches were on November 22-23, 1977. The sky was overcast with ground fog or heavy haze. Low altitude wind was from the east (from the ocean). After launch, the flight train went inland slowly until it reached 10,000 feet when the wind reversed to the west. The sonde came back over the station and went out to sea. Winds aloft were 100 to 150 knots. Near the end of the flight, the sonde was only 6 to 8 degrees above the horizon because of the strong winds aloft. There was severe fading of the telemetry signal, probably due to multipath interference over the ocean. Launch data is shown in Table 1.



Figure 6. Honeywell Ground Support Equipment in the Met-Ops Building

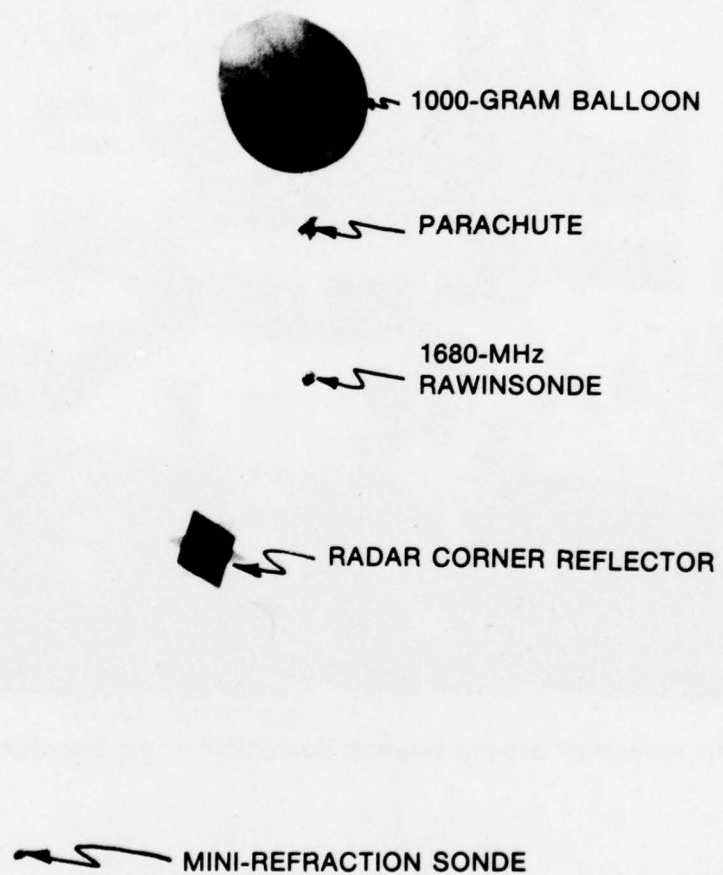


Figure 7. Sonde Launch Flight Train

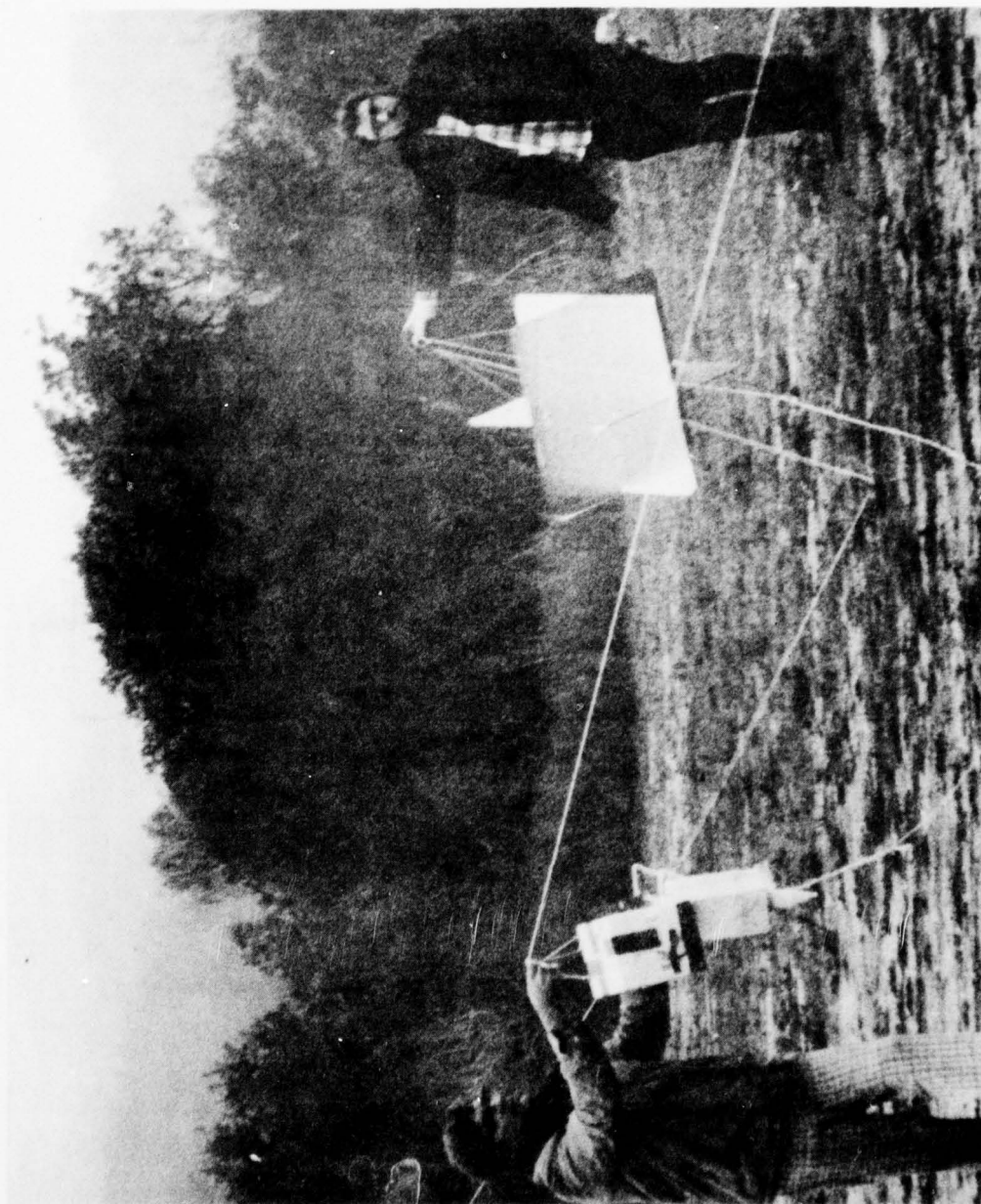


Figure 8. Radar Corner Reflector

Table 1. Launch Data

Flight Number	1	2	3
Sonde Serial Number	11	10	9
Launch Date	11-22-77	11-23-77	11-23-77
Launch Time (EST)	2:30 p.m.	10:20 a.m.	2:00 p.m.
Balloon Size (gms)	600	2000	600
Transmitter Frequency (MHz)	404.3	404.5	403.6
Record Tape Number	1	2 and 3	4 and 5
Launch Pressure (mB)	1031.3	1024.9	1020.4
Launch Temperature (°C)	6.7	9.4	11.1

III. Test Results

The purpose of this test was to make a preliminary demonstration of operation of the Mini-Refracton Sonde under actual flight conditions. The three flights were very successful and much was learned. All three sondes operated and continued to transmit data for one to two hours. This corresponds to an altitude greater than 100,000 feet and temperatures below -60°C .

Since there was no on-line processor available to reduce the sonde data, the received telemetry signals were recorded on a four-channel, analog, FM magnetic tape recorder for later processing. These five tapes were returned to Honeywell's Hopkins, Minnesota, facility for processing. The Honeywell Data Laboratory facilities were used as described in the previous report, NADC 76129-30, "Miniature Meteorological Balloonsonde." This laboratory system consists of a digitizer to measure the period of the telemetered data and a Honeywell 516 Minicomputer to calculate temperature, pressure and humidity.

The flights were also tracked with radar to provide a measurement of altitude versus time.

Each minisonde was attached to the flight train of a NWS Rawinsonde launch, and a copy of the Rawinsonde data was provided to us by NASA. Since the Rawinsonde telemetry signal was recorded on one channel of the tape recorder, it was possible to compare altitude measurements of the Mini-Refracton Sonde with the contact numbers of the Rawinsonde.

A listing of this total data set is shown in the table in each flight section. Time is the common baseline of comparison. The tables list radar altitude, Rawinsonde readings and Mini-Refracton Sonde (MRS) readings.

During the early part of the first flight, telemetry difficulties were encountered because of the remote placement of the dipole antenna and high cable loss. When the receiver was switched to the UHF antenna with an antenna-mounted preamplifier, the signal cleared. This problem reduced the quality of the recorded Mini-Refracton Sonde signal for flight one.

The second launch was in conjunction with an ozone sonde launch. To measure ozone, a Rawinsonde was modified to time commutate a frequency signal from the ozone sensor. This made it impossible to identify the exact contact points of the Rawinsonde. It was not possible to make exact comparison between the Mini-Refracton Sonde and Rawinsonde pressure and altitude data.

Because of the difficulties with the first two flights, only flight number three represents the best flight comparison. Results of flight three should be representative of the present sonde performance.

A. FLIGHT NUMBER ONE

A listing of all the flight data is shown in Table 2. Greenwich Mean Time (GMT) is shown in column one to compare with the radar track. Column two gives time after launch in minutes and seconds. Column three lists the NWS Rawinsonde baroswitch contact points and column seven shows the pressure corresponding to each contact number. In columns four, five and six are shown the sonde altitude versus time as tracked by radar, read by the NWS sonde and read by the Mini-Refraction Sonde. Columns 7 through 12 give the readings of pressure, temperature and humidity read by the NWS Rawinsonde and the Mini-Refraction Sonde. The last four columns on the right, 13 through 16, show the calculated values of N and M for the modified refractive index. All of this data is plotted in the following figures.

Plots of sonde altitude versus time are shown in Figures 9 through 11 for the Mini-Refraction Sonde (MRS), National Weather Service Rawinsonde (NWS) and radar. These three plots follow so closely to each other that they cannot be plotted on a single graph and still be separated. To illustrate the variation between altitude readings, the NWS altitude and the MRS altitude were subtracted from the NASA radar-measured altitude and plotted in Figure 12. Over the first 7 kilometers (20,000 feet) the readings agree within 60 meters.

There is no apparent reason for the deviation in altitude reading by the Mini-Refraction Sonde above 7 kilometers. This does not appear in the other two flights.

A plot of free-air temperature versus altitude for the NWS Rawinsonde and the Mini-Refraction Sonde (MRS) is shown in Figure 13. The two readings agree closely. There is no systematic error apparent. Note that there are two inversion layers indicated in the data at 1 and 3 kilometers. For some reason, the minisonde responded to the 3 kilometer inversion more quickly than the NWS sonde.

The measured humidity profile is plotted in Figure 14. The humidity readings by the NWS sonde and minisonde agree within the hygistor accuracy. The readings differ by 10 percent relative humidity above 9 kilometers, but the free-air temperature at this level is below -40°C , causing the hygistor response to fall off.

The modified refractive index, N, and M-units are plotted versus altitude in Figure 15. Although the data is plotted to 12 kilometers, most of the index variations are at 3 kilometers and below.

Table 2. Flight Data for Flight Number 1, Sonde Number 11

Time GMT	Time T ₀ + M S	NWS Baro. Cont.	NASA Radar Alt. -M	NWS Alt. -M	MRS Alt. -M	NWS Press. mb δ	MRS Press. mb δ	NWS Temp. °C	MRS Temp. °C	NWS R. H. %	MRS R. H. %	NWS Refr. Index		MRS Refr. Index	
												N	M	N	M
19:37:37	00:09	4	74		62.6	1028.6	1022.1	5.8	7.5	77.3	82.0	320.5	332.8	322.8	334.9
19:38:04	00:36	5	161		168.2	1014.8	1008.1	4.5	6.4	-	87.5	318.5	347.2	320.3	348.7
19:38:31	01:03	6	268		267.6	1001.0	996.0	5.5	6.4	91.2	93.6	317.2	362.7	318.3	363.3
19:38:55	01:27	7	372		373.9	987.4	983.9	4.7	5.3	92.4	95.3	313.6	374.8	315.1	375.5
19:39:22	01:54	8	495		501.3	974.6	968.9	4.6	4.7	67.1	72.2	298.3	379.1	300.4	380.4
19:39:46	02:18	9	608		618.5	961.2	956.5	4.5	4.6	68.0	71.8	295.0	392.4	296.7	392.9
19:40:10	02:42	10	722		720.2	948.4	943.7	4.6	4.9	-	78.3	296.2	413.0	296.2	409.6
19:40:34	03:06	11	835			935.4	931.9	6.3	6.2	96.3	98.2	302.9	434.3	303.5	433.3
19:41:01	03:33	12	967	806	948.2	922.8	918.5	8.2	8.5	96.6	97.6	303.3	454.0	303.1	452.0
19:41:28	04:00	13	1089			910.2	905.5	9.8	10.0	96.6	97.6	303.4	473.1	303.9	471.6
19:41:52	04:24	14	1193		1163.5	897.6	894.0	9.8	10.2	96.6	96.9	300.7	487.1	300.9	485.1
19:42:19	04:51	15	1311		1267.4	885.4	882.9	9.3	9.8	-	95.8	296.9	498.4	296.4	496.4
19:42:43	05:15	16	1412		1403.7	873.4	868.6	8.6	9.2	97.5	98.1	291.8	515.3	292.2	513.0
19:43:07	05:39	17	1511		1512.5	861.0	857.3	7.9	8.6	97.6	97.9	287.4	527.6	287.6	525.0
19:43:34	06:06	18	1635		1610.0	849.2	845.7	7.5	8.4	95.8	91.6	282.8	540.5	280.8	535.4
19:43:58	06:30	19	1743		1750.9	837.2	832.9	7.0	7.5	94.6	92.2	276.7	553.8	275.6	549.2
19:44:25	06:57	20	1875		1886.0	825.4	821.1	6.2	6.7	-	93.6	271.8	566.8	271.5	563.0
19:44:52	07:24	21	2011		1979.0	813.8	809.4	5.6	6.0	95.0	95.3	267.7	580.9	267.7	577.1
19:45:16	07:48	22	2124		2232.8	802.0	797.9	4.7	5.4	90.2	95.9	263.3	594.5	263.7	591.0
19:45:40	08:12	23	2230		2348.4	790.8	785.9	4.3	5.0	94.5	94.9	259.0	609.5	259.2	605.4
19:46:07	08:39	24	2352		2472.8	779.4	774.4	3.8	4.4	94.4	94.8	254.7	623.8	255.0	619.5
19:46:43	09:15	25	2520		2587.4	768.0	763.0	3.0	3.7	-	95.5	250.7	638.4	250.9	633.8
19:47:01	09:33	26	2591		2701.8	757.0	752.0	2.3	2.8	96.0	95.7	246.6	652.2	246.5	647.2
19:47:25	09:57	27	2701		2715.8	746.0	740.2	1.2	2.6	67.5	69.2	232.7	658.4	233.4	653.7
19:47:49	10:21	28	2825			735.0	730.3	1.5	4.8	15.0	19.5	210.1	654.2	212.0	650.7
19:48:13	10:45	29	2945		2967.3	724.4	718.9	3.1	4.5	54.5	58.5	223.2	687.8	224.8	683.7
19:48:37	11:09	30	3061		3079.1	713.6	707.9	2.8	3.5	-	64.5	223.2	708.8	223.2	700.9
19:49:04	11:36	31	3201		3207.1	703.0	696.8	3.4	2.5	85.0	80.2	226.8	729.9	225.0	722.0
19:49:28	12:00	32	3324	3267	3329.2	692.2	686.4	1.4	1.7	83.0	84.9	222.1	743.6	222.8	738.0
19:49:52	12:24	33	3392	3408	3454.2	680.2	675.8	0.2	0.7	48.0	56.1	206.8	746.9	209.4	743.0
19:50:19	12:51	34	3569		3590.6	669.8	664.4	-0.5	0.5	64.3	66.6	208.7	770.4	209.5	764.4
19:50:43	13:15	35	3688		3701.0	659.8	655.3	-0.8	-0.1	-	41.4	196.8	775.3	198.8	770.1
19:51:13	13:45	36	3836		3840.2	649.4	644.0	-2.0	-0.9	16.0	22.9	188.1	787.6	190.2	782.3
19:51:37	14:09	37	3950		3959.5	639.2	634.5	-2.3	-1.3	16.0	8.8	185.6	803.5	183.6	793.9

Table 2. Flight Data for Flight Number 1, Sonde Number 11 (Continued)

TIME GMT	TIME T + M S	NWS Baro. Cont.	NASA Radar Alt-M	NWS Alt-M	MRS Alt-M	NWS Press. mb	MRS Press. mb	NWS Temp. °C	MRS Temp. °C	NWS R.H. %	MRS R.H. %	NWS Refr. Index			MRS Refr. Index		
												N	M	N	N	M	N
19:52:04	14:36	38	4088		4087.2	629.0	624.4	-2.7	-1.7	<10.0	7.0	181.2	819.0	180.4		810.4	
19:52:28	15:00	39	4215		4210.3	619.0	614.0	-2.6	-1.6	<10.0	7.9	178.2	837.5	177.6		828.8	
19:52:52	15:24	40	4334	4156	4360.9	609.4	604.7	-3.0	-2.0	-	8.5	175.7	853.9	175.3		845.1	
19:53:19	15:51	41	4479		4470.9	599.6	594.9	-3.8	-2.6	<10.0	9.3	173.2	871.3	173.0		862.5	
19:53:46	16:18	42	4614		4599.0	589.8	584.5	-5.0	-4.0	<10.0	9.9	170.8	889.5	170.8		880.6	
19:54:13	16:45	43	4745		4725.2	580.2	575.1	-6.1	-5.2	11.0	10.8	168.9	906.4	168.9		897.3	
19:54:37	17:09	44	4865			570.6	565.5	-7.0	-6.3	13.0	13.9	167.0	924.3	167.2		915.1	
19:55:04	17:36	45	4994		5000.9	561.4	556.5	-7.6	-6.8		10.5	164.0	941.0	164.2		931.2	
19:55:28	18:00	46	5119		5129.5	552.2	547.0	-8.3	-7.4	10.0	10.3	161.5	959.1	161.6		949.2	
19:55:55	18:27	47	5241	5054	5259.6	543.2	538.0	-9.0	-8.2	10.0	10.3	159.3	976.5	159.4		966.5	
19:56:22	18:54	48	5377		5396.4	533.4	528.5	-10.1	-9.3	10.0	10.7	157.0	994.9	157.2		984.5	
19:56:52	19:24	49	5520		5511.0	525.0	520.0	-11.1	-10.2	10.0	10.4	154.9	1011.7	155.0		1001.0	
19:57:19	19:51	50	5659		5643.3	516.4	511.3	-12.3	-11.3		10.3	152.9	1028.9	153.0		1018.1	
19:57:46	20:18	51	5794		5930.3	507.4	501.7	-13.1	-12.7	<10.0	10.6	150.8	1048.0	150.8		1036.9	
19:58:10	20:42	52	5910		6051.5	498.8	493.0	-14.5	-13.9	10.0	11.1	148.6	1065.9	148.8		1054.4	
19:58:37	21:09	53	6047		6201.0	490.4	485.2	-15.7	-15.0	10.0	10.9	146.9	1081.7	147.0		1070.2	
19:59:04	21:36	54	6189			481.8	476.2	-16.4	-15.6	11.0	11.3	144.6	1101.7	144.6		1089.7	
19:59:31	22:03	55	6309			473.6	468.0	-17.4	-16.5		12.3	142.6	1119.6	142.7		1107.3	
20:00:01	22:33	56	6453		6461.2	465.4	459.9	-18.2	-17.6	12.0	12.9	140.7	1137.2	140.8		1124.7	
20:00:25	22:57	57	6588		6591.6	457.0	451.5	-18.7	-18.1	12.0	12.9	138.4	1156.6	138.5		1143.7	
20:00:49	23:21	58	6725		6736.5	448.8	442.2	-19.6	-19.1	12.0	12.9	135.9	1178.1	136.1		1164.7	
20:01:13	23:45	59	6848		6880.6	441.0	434.4	-20.9	-20.2	12.0	12.5	134.1	1195.8	134.1		1182.5	
20:01:40	24:12	60	6989		7019.3	433.0	426.3	-22.0	-21.1		12.7	132.0	1215.0	132.1		1201.3	
20:02:04	24:36	61	7135			425.2	418.7	-22.6	-21.8	12.5	12.1	130.1	1233.4	130.0		1219.5	
20:02:28	25:00	62	7266		7284.9	417.4	411.2	-23.1	-22.3	12.0	12.3	127.9	1252.5	127.9		1238.2	
20:02:55	25:27	63	7404			410.4	403.5	-24.4	-23.5	12.0	11.7	126.1	1271.2	126.1		1256.5	
20:03:22	25:54	64	7554		7566.1	402.2	395.7	-25.8	-24.8	12.0	11.8	124.2	1290.4	124.2		1275.3	
20:03:49	26:21	65	7677		7721.6	394.8	387.7	-26.8	-25.7	12.5	12.6	122.1	1311.0	122.1		1295.7	
20:04:19	26:51	66	7814		7843.1	387.2	380.5	-27.9	-27.1	12.5	12.6	120.5	1328.9	120.5		1313.5	
20:04:49	27:21	67	7959		7986.6	380.2	373.3	-29.1	-28.1	12.5	13.2	118.7	1347.9	118.7		1331.9	
20:05:16	27:48	68	8101		8125.9	372.8	366.1	-30.2	-29.3	13.0	13.1	116.9	1366.8	117.0		1350.5	
20:05:43	28:15	69	8230		8265.8	365.6	359.0	-31.0	-30.0	12.5	12.9	114.9	1386.8	115.0		1370.2	
20:06:10	28:42	70	8348		8412.1	358.4	351.7	-32.2	-31.2		13.6	113.1	1406.7	113.2		1389.8	
20:06:40	29:12	71	8506		8554.2	351.4	344.7	-33.1	-32.3	13.0	13.7	111.4	1426.4	111.4		1409.2	

Table 2. Flight Data for Flight Number 1, Sonde Number 11 (Concluded)

TIME GMT	TIME T. + M S	NWS Baro. Cont.	NASA Radar Alt-M	NWS Alt-M	MRS Alt-M	NWS Press. mb	MRS Press mb	NWS Temp. °C	MRS Temp. °C	NWS R.H. %	MRS R.H. %	NWS Refr. Index		MRS Refr. Index	
												N	M	N	M
20:07:07	29:39	72	8647		8707.1	344.2	338.0	-33.8	-32.9	13.0	13.2	109.5	1446.5	109.5	1429.0
20:07:34	30:06	73	8764		8853.7	337.6	330.4	-34.7	-34.0	13.0	13.3	107.5	1468.8	107.5	1451.1
20:08:01	30:33	74	8915		9001.4	330.8	324.1	-35.7	-34.8	13.5	14.4	105.8	1488.0	105.8	1469.9
20:08:25	30:57	75	9046			324.2	317.1	-36.7	-35.7	-	14.0	103.9	1510.0	103.9	1491.3
20:08:52	31:24	76	9193	9091	9267.2	317.6	310.7	-38.0	-37.1	17.0	16.5	102.4	1528.9	102.4	1510.0
20:09:22	31:54	77	9353		9419.7	311.0	304.2	-39.0	-38.4	27.0	22.0	100.9	1549.0	100.9	1529.4
20:09:49	32:21	78	9497		9554.8	304.2	298.0	-40.0	-39.2	40.5	34.6	99.4	1569.3	99.4	1549.9
20:10:16	32:48	79	9635		9716.3	298.2	291.6	-41.1	-40.1	47.5	45.6	97.7	1590.7	97.7	1570.8
20:10:43	33:15	80	9769		9877.4	292.0	285.6	-42.1	-41.1	51.0	51.4	96.1	1610.4	96.1	1590.7
20:11:10	33:42	81	9904			285.8	280.0	-43.2	-42.1	53.0	53.3	94.3	1632.9	94.3	1608.9
20:11:34	34:06	82	10025	9956	10149.0	279.6	273.6	-44.2	-43.5	53.0	56.5	92.9	1650.8	93.0	1630.2
20:12:01	34:33	83	10162			273.6	267.0	-45.5	-44.6	52.5	57.3	91.0	1674.5	91.1	1653.2
20:12:28	35:00	84	10318		10461.6	267.6	261.6	-46.5	-45.5	52.4	57.2	89.5	1693.8	89.6	1672.5
20:12:49	35:21	85	10439			261.8	256.0	-47.6	-46.2	-	56.2	87.9	1714.9	87.9	1693.5
20:13:29	35:51	86	10648		10781.3	256.2	249.9	-48.6	-47.4	52.5	56.7	86.2	1737.4	86.2	1715.7
20:13:49	36:21	87	10747		10900.2	250.4	244.4	-50.0	-48.7	48.0	53.6	84.7	1757.9	84.8	1735.2
20:14:19	36:51	88	10895		11051.0	244.6	238.7	-51.2	-49.7	46.0	50.5	83.1	1780.3	83.2	1757.2
20:14:46	37:18	89	11028		11197.8	238.8	234.0	-52.3	-51.7	45.0	49.3	82.2	1795.5	82.2	1772.4
20:15:16	37:48	90	11178		11346.9	233.6	228.2	-53.5	-52.5	-	47.9	80.4	1820.0	80.4	1796.4
20:15:43	38:15	91	11315		11486.7	228.2	223.1	-54.9	-53.7	42.5	47.2	79.0	1840.4	79.1	1816.4
20:16:13	38:45	92	11460		11636.4	223.0	218.2	-55.7	-54.5	42.0	46.8	77.5	1861.6	77.6	1837.3
20:16:43	39:15	93	11592		11784.0	217.8	213.2	-56.5	-55.3	42.0	46.4	76.0	1883.9	76.1	1859.1
20:17:16	39:48	94	11752		11954.1	212.8	207.6	-56.5	-55.3	42.0	46.4	74.0	1912.4	74.1	1887.3
20:17:46	40:18	95	11903		12101.9	207.8	202.6	-56.9	-55.8	-	45.8	72.4	1936.8	72.4	1911.6
20:18:16	40:48	96	12048		12261.2	202.8	197.8	-57.6	-56.2	41.0	45.5	70.9	1960.8	70.9	1935.2
20:18:49	41:21	97	12202		12413.4	198.0	193.3	-58.3	-57.2	40.0	44.9	69.6	1981.3	69.5	1956.4
20:19:19	41:51	98	12344		12573.0	193.0	188.5	-59.3	-57.7	40.0	44.9	68.0	2007.6	68.0	1981.0

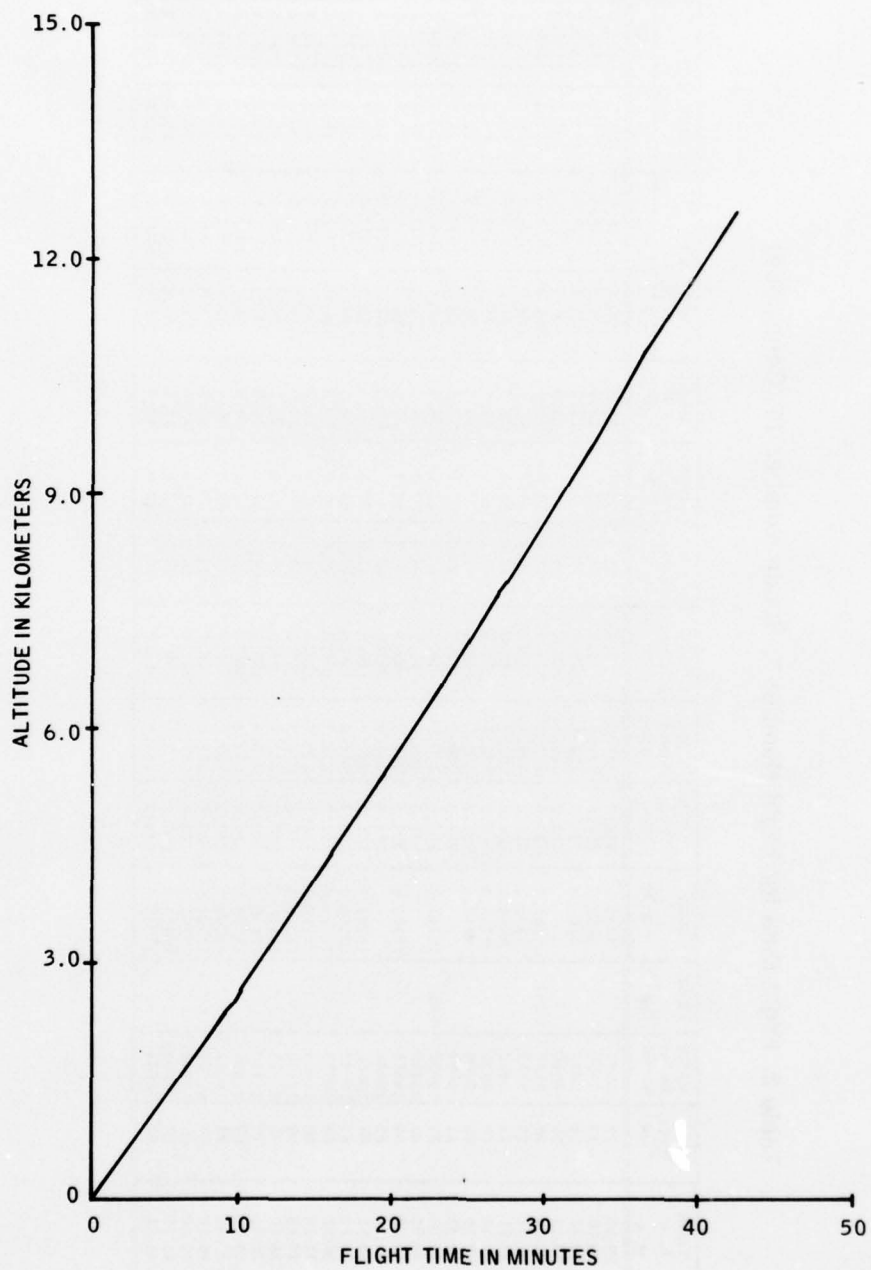


Figure 9. Plot of Altitude versus Time Measured with Mini-Refraction Sonde — Flight Number 1

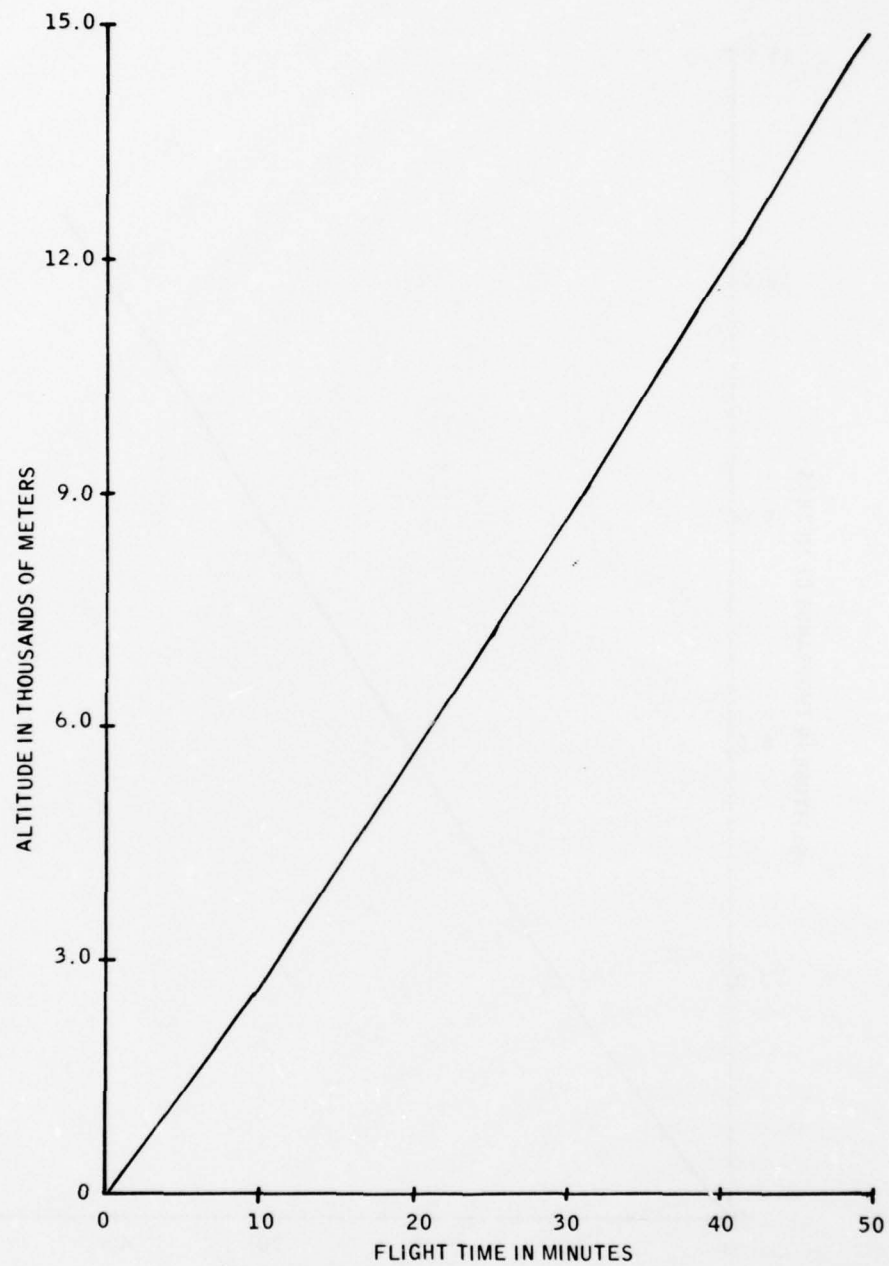


Figure 10. Plot of Altitude versus Time Measured with NWS Rawinsonde — Flight Number 1

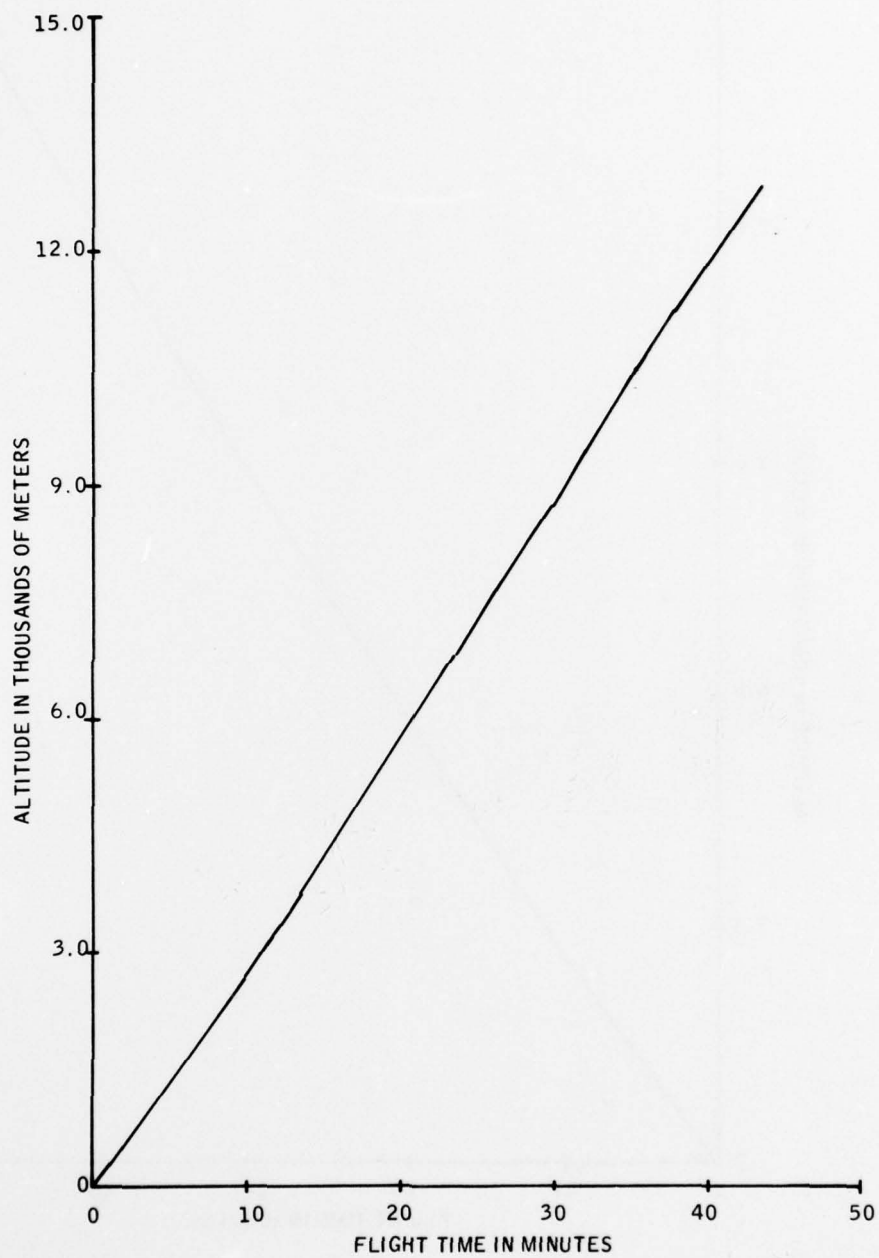


Figure 11. Plot of Altitude versus Time Measured with NASA Radar — Flight Number 1

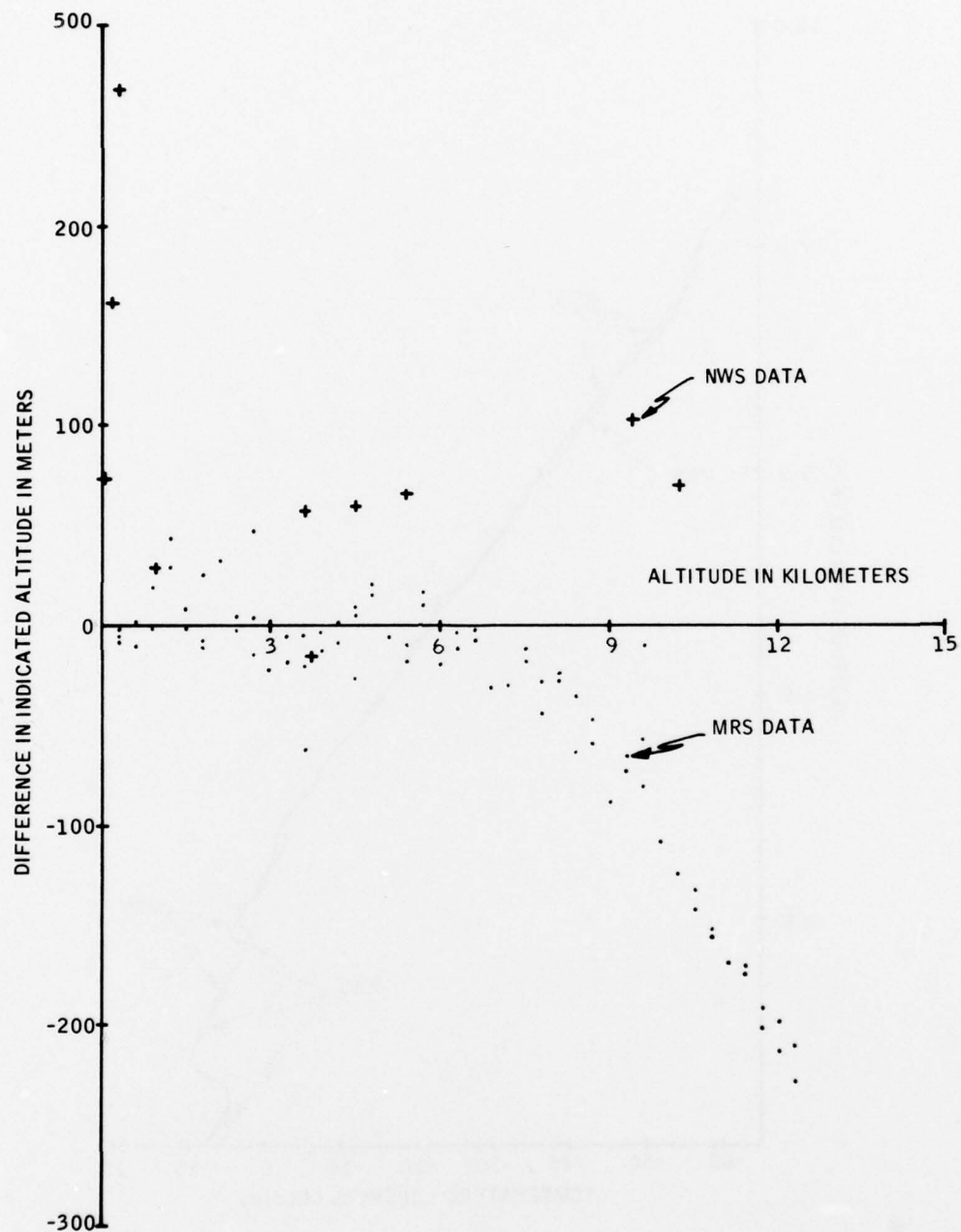


Figure 12. Plot of Difference in Altitude Reading of the MRS and Rawinsonde versus Radar — Flight Number 1

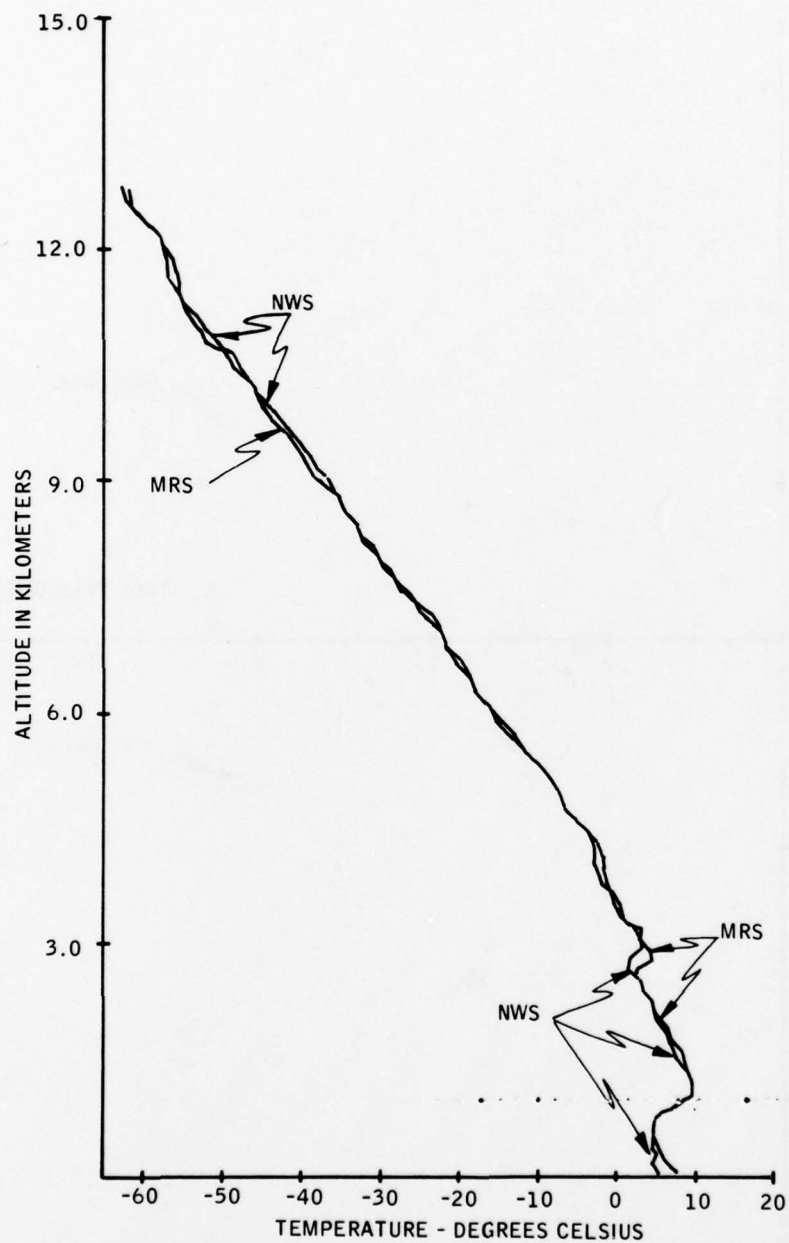


Figure 13. Plot of Free-Air Temperature versus Altitude for the MRS and Rawinsonde — Flight Number 1

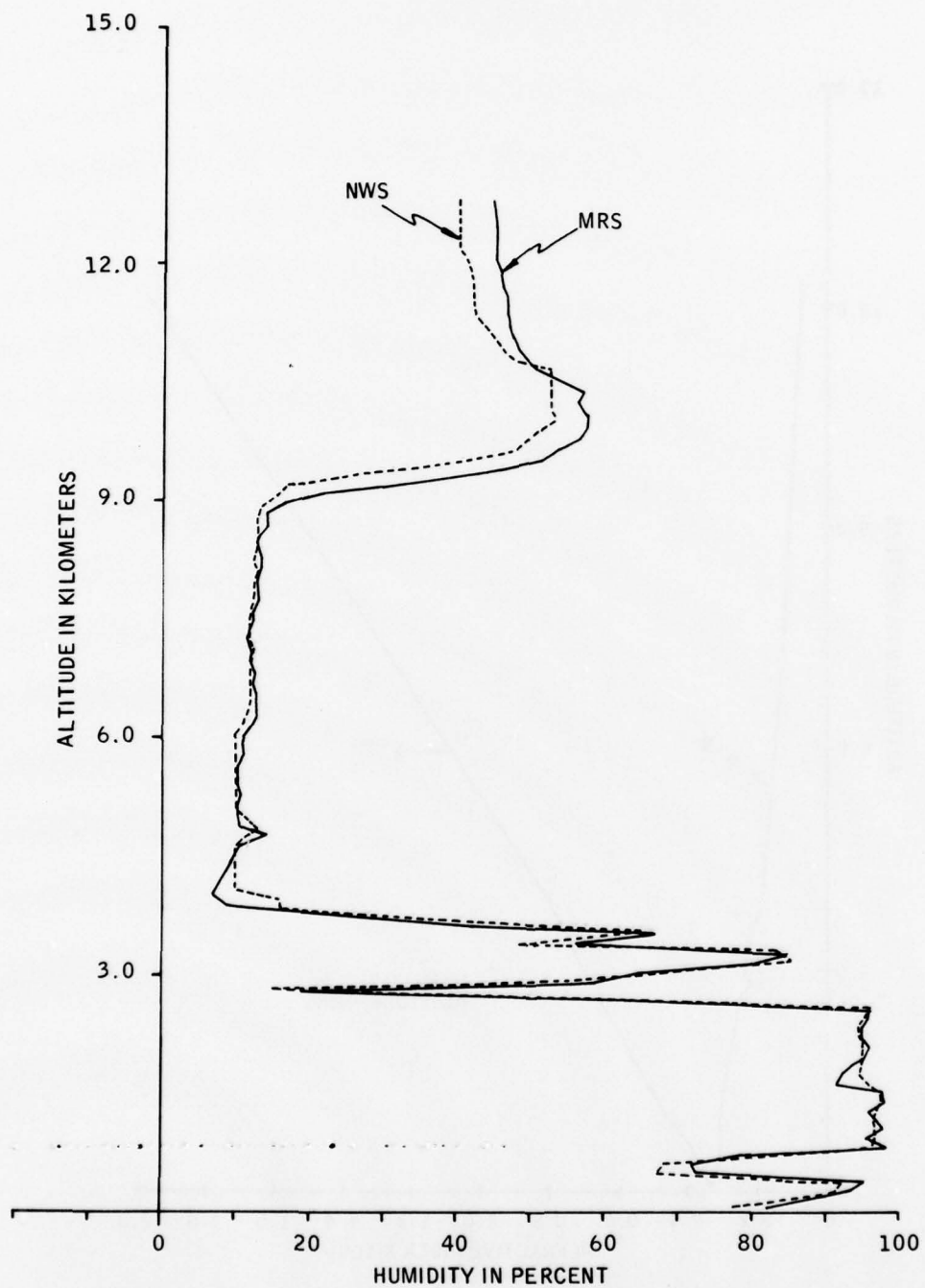


Figure 14. Plot of Relative Humidity versus Altitude for the MRS and Rawinsonde — Flight Number 1

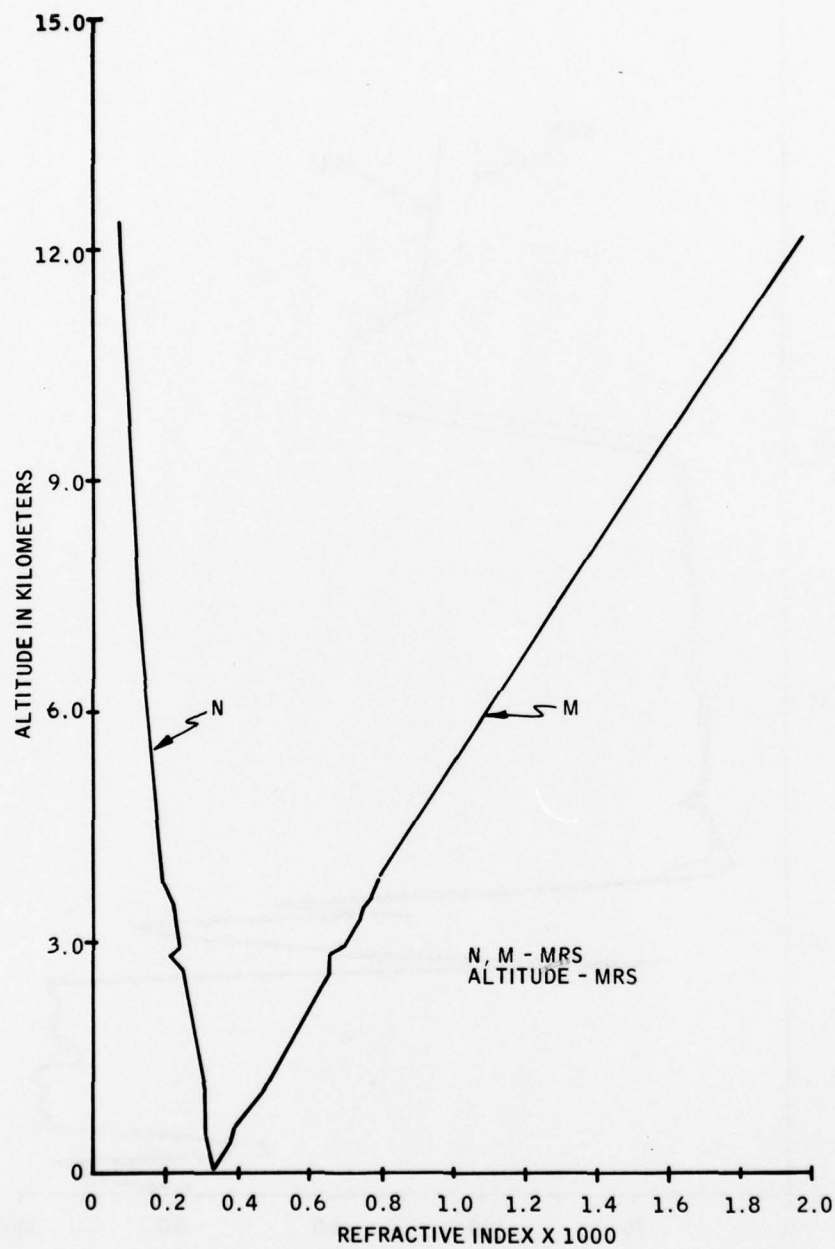


Figure 15. Plot of Modified Refractive Index, N, and M-Units versus Altitude Read by Mini-Refraction Sonde — Flight Number 1

B. FLIGHT NUMBER TWO

A listing of all the flight number 2 data is shown in Table 3. The flight was an ozone-Rawinsonde sounding which inserted ozone readings into the Rawinsonde data stream. These periodic interruptions to the regular barometric commutation made it impossible to exactly correlate the Rawinsonde pressure readings with the Mini-Refraction Sonde readings. The rest of the columns are as described in Table 2. A separate listing of Rawinsonde altitude versus radar-tracked altitude is shown in Table 4.

Plots of altitude versus time are shown in Figures 16 through 18 for the MRS, NWS and radar. These plots are very close, as can be seen from the data in Tables 3 and 4.

A plot of measured free-air temperature versus altitude for the Rawinsonde and MRS is shown in Figure 19. The Mini-Refraction Sonde is reading about 3°C higher in temperature than the Rawinsonde. Both indicate the same temperature trend and show a small inversion at 2800 meters. This offset could be caused by self-heating or a thermal lag in the MRS thermistor mounting chamber. It could also be due to a calibration error in one of the thermistors.

The measured humidity profile is plotted in Figure 20. Although the trend of the curves agrees well, the Rawinsonde indicates significantly lower humidities when reading less than 33 percent. At these humidities, the carbon hygistor has minimum resistance. Possibly the MRS hygistor mount was not making good contact with the hygistor. The mounts could be gold- or silver-plated in future models. It is also possible that the hygistor was damaged while being inserted due to operator inexperience.

The modified refractive index, N, and M-units are plotted versus altitude in Figure 21. The curves are almost straight, indicating no significant ducting.

Table 3. Flight Data for Flight Number 2, Sonde Number 10

Time GMT H M S	Time To + M S	NWS Baro. Cont.	NASA Radar Alt - M	NWS Alt - M	MRS Alt - M	NWS Press. mb	MRS Press. mb	NWS Temp. °C	MRS Temp. °C	NWS R. H. %	MRS R. H. %	NWS Refr. Index		MRS Refr. Index	
												N	M	N	M
15:20:21	00:36	5			123.9	1012.2	1010.5	12.0	12.0	90.3	90.3			333.3	352.1
:	:	6			230.0	1000.6	998.7	13.5	13.5	91.4	91.4			334.8	379.2
:	:	7			304.8	988.8	987.9	13.2	13.2	90.4	90.4			330.3	378.5
:	:	8			403.0	977.6	976.8	13.1	13.1	90.4	90.4			326.9	389.6
15:22:15	02:30	9			506.7	966.0	964.9	12.7	12.7	90.5	90.5			322.8	401.3
15:22:39	02:54	10				955.2	954.2	13.1	13.1	90.3	90.3			320.8	413.8
:	:	11				943.6	943.8	14.9	14.9	90.7	90.7			323.4	431.0
:	:	12		692		932.8	932.0	14.8	14.8	90.6	90.6			319.9	443.8
:	:	13				921.6	920.5	14.2	14.2	90.6	90.6			315.1	454.9
15:24:21	04:36	14			988.6	910.4	911.5	14.1	14.1	90.4	90.4			312.0	464.5
:	:	15			1104.2	900.0	899.0	13.5	13.5	90.4	90.4			307.1	477.3
:	:	16			1193.8	889.0	888.8	12.7	12.7	90.5	90.5			302.2	486.9
:	:	17			1275.8	878.2	879.3	12.2	12.2	90.6	90.6			298.3	496.7
:	:	18			1423.4	867.6	866.9	11.4	11.4	90.4	90.4			292.7	509.1
:	:	19			1516.5	856.6	855.8	10.9	10.9	90.6	90.6			288.6	521.5
15:25:57	06:12	20			1599.5	846.4	845.7	10.4	10.4	90.6	90.6			284.5	532.2
:	:	21			1738.3	835.6	834.8	9.4	9.4	90.7	90.7			279.3	543.2
:	:	22			1835.6	825.2	824.4	9.1	9.1	90.7	90.7			275.7	555.6
:	:	23			1947.1	815.2	814.4	8.3	8.3	90.7	90.7			271.4	566.5
15:27:27	07:42	24			2156.0	805.0	804.2	7.6	7.6	90.8	90.8			267.2	577.9
:	:	25			2263.9	794.8	793.3	6.6	6.6	90.8	90.8			262.3	589.9
:	:	26			2373.3	784.0	783.5	6.2	6.2	90.8	90.8			258.9	602.2
:	:	27			2452.0	774.0	772.7	5.8	5.8	90.9	90.9			255.1	615.8
:	:	28			2577.8	764.4	764.4	5.2	5.2	91.0	91.0			251.8	625.8
15:28:42	08:57	29			2695.7	754.2	752.7	4.6	4.6	91.0	91.0			247.6	640.8
15:29:03	09:18	30			2804.1	744.4	743.0	4.2	4.2	91.1	91.1			244.2	654.7
15:29:51	10:06	31		2756	2866	734.6	733.0	-2.2	-2.2	51.7	51.7			225.2	650.5
:	:	32				725.0	725.0	3.8	3.8	31.3	31.3			215.6	657.7
:	:	33				715.2	715.7	6.6	6.6	49.4	49.4			222.3	682.0
:	:	34			3129.1	705.4	703.5	7.7	7.7	31.9	31.9			210.0	690.4
15:31:24	11:39	35			3258.7	696.0	694.0	6.2	6.2	30.1	30.1			206.4	703.7
:	:	36			3349.7	686.2	685.0	5.8	5.8	33.4	33.4			208.0	721.7
:	:	37			3461.1	676.8	675.4	5.5	5.5	33.2	33.2			202.5	733.7
:	:	38			3599.6	667.2	665.6	4.7	4.7	33.4	33.4			199.7	748.8

Table 3. Flight Data for Flight Number 2, Sonde Number 10 (Continued)

Time GMT H M S	Time To + M S	NWS Baro Cont.	NASA Radar Alt - M	NWS Alt - M	MRS Alt - M	NWS Press. mb	MRS Press. mb	NWS Temp. °C	MRS Temp. °C	NWS R. H. %	MRS R. H. %	NWS Refr. Index		MRS Refr. Index	
												N	M	N	M
:	:	39			3697.6	657.8	656.5		4.0		29.9			195.6	761.5
:	13:33	40			3824.3	646.8	646.8		3.1		29.8			192.8	776.5
:	:	41			3913.5	639.6	638.6		2.6		28.3			190.0	789.2
:	:	42			4047.8	630.4	628.5		2.5		30.7			188.0	807.4
:	:	43			4161.9	621.4	619.9		1.5		32.1			186.0	821.8
:	:	44			4268.8	612.4	611.1		0.6		31.9			183.4	836.0
:	15:39	45			4406.0	603.2	601.3		-0.2		31.2			180.3	852.4
:	:	46			4506.7	594.2	594.1		-0.5		29.5			177.8	864.6
:	:	47			4647.4	585.4	583.5		-0.9		30.8			175.2	884.2
:	:	48			4755.9	577.0	575.0		-1.4		29.0			172.3	896.9
:	:	49			4859.3	568.4	566.5		-1.9		29.1			169.9	914.6
:	17:54	50			5013.6	559.6	556.4		-3.1		29.2			167.1	932.7
:	:	51			5150.6	551.2	548.3		-4.0		31.0			165.3	948.1
:	:	52			5243.0	542.4	541.1		-4.7		30.5			163.2	961.3
:	:	53			5366.6	534.2	532.9		-5.3		31.9			161.2	977.4
:	:	54			5488.8	525.8	525.0		-6.4		31.5			159.0	992.3
:	20:00	55	5600		5643.3	517.4	514.4		-7.6		31.8			156.1	1012.8
:	:	56			5774.7	509.2	506.0		-8.3		29.3			153.3	1029.2
:	:	57			5889.9	501.2	498.7		-8.4		28.4			151.1	1044.7
:	:	58			5981.0	493.0	492.5		-9.1		28.8			149.5	1057.7
:	:	59			6101.3	485.0	484.7		-9.8		31.5			147.8	1074.3
:	22:03	60			6258.2	477.0	476.0		-10.8		35.9			146.0	1093.3
:	22:24	61		6292	6387.4	469.0	467.3		-11.7		45.1			144.8	1113.3
:	:	62			6531.3	460.2	458.3		-13.0		58.5			143.9	1134.1
:	:	63			6651.6	452.6	451.2		-14.0		68.0			142.9	1150.5
:	:	64			6797.5	444.8	442.5		-15.2		76.3			141.1	1170.2
:	24:03	65		6942	6927.3	437.2	435.0		-16.2		83.4			139.6	1189.2
:	24:36	66			7084.9	429.6	428.0		-15.6		53.5			133.9	1207.2
:	:	67			7196.0	422.2	419.9		-15.6		47.8			131.4	1223.6
:	:	68			7311.9	414.8	413.0		-15.8		48.1			129.4	1241.6
:	:	69			7443.5	408.0	406.7		-16.2		39.5			126.7	1256.6
:	26:18	70			7576.6	400.6	399.1		-17.6		38.6			124.6	1274.6
:	:	71			7695.1	393.2	392.6		-18.2		37.1			122.6	1291.2
:	:	72			7839.4	386.2	385.3		-18.8		35.3			120.4	1310.4

Table 3. Flight Data for Flight Number 2, Sonde Number 10 (Concluded)

Time GMT H M S	Time To + M S	NWS Baro Cont.	NASA Radar Alt - M	NWS Alt - M	MRS Alt - M	NWS Press. mb	MRS Press. mb	NWS Temp °C	MRS Temp °C	NWS R. H. %	MRS R. H. %	NWS Refr. Index		MRS Refr. Index	
												N	M	N	M
:	:	73		8001.2	7731.1	379.0	377.0		-20.0		33.2			118.0	1331.8
:	:	74		8140.5	7858.2	372.0	369.6		-21.8		35.3			116.3	1350.1
:	28:39	75		8299.6	7997.4	365.2	362.5		-22.4		36.5			114.4	1370.0
:	:	76		8426.1	8115.9	358.6	355.8		-24.0		37.9			112.8	1387.0
:	:	77		8560.1	8244.2	351.6	348.5		-24.6		34.8			110.8	1405.2
:	:	78		8691.9	8363.8	345.0	343.2		-25.8		35.9			109.3	1422.4
:	:	79		8846.6	8508.5	338.2	335.9		-26.9		35.6			107.3	1443.2
:	30:57	80		8978.7	8625.8	332.0	328.7		-28.5		36.2			105.9	1460.1
:	:	81		9080.3	8722.5	325.4	325.0		-29.2		38.8			104.7	1474.1
:	:	82		9258.4	8889.8	319.0	317.0		-30.4		36.9			102.5	1498.2
:	:	83		9402.8	9027.7	312.6	310.4		-31.7		36.2			100.7	1518.1
:	33:15	84		9539.3	9173.8	306.2	304.1		-32.2		33.8			98.8	1539.1
:	:	85		9692.0	9306.4	300.4	296.1		-33.2		34.6			97.2	1558.3
:	:	86		9848.6	9437.5	294.0	291.6		-35.1		39.6			95.8	1577.5
:	:	87		9984.9	9567.8	288.2	285.8		-36.1		45.5			94.4	1596.6
:	:	88		10145.1	9712.7	282.2	279.4		-37.5		45.8			92.7	1617.6
:	35:12	89		10232.9	9808.2	276.4	275.5		-38.0		44.5			91.6	1631.5
:	:	90		10403.2	9945.7	270.6	268.1		-39.9		44.8			90.1	1651.6
:	:	91		10559.1	10093.7	264.8	263.0		-41.0		45.8			88.4	1673.2
:	:	92		10716.3	10240.4	259.2	257.1		-42.0		44.4			86.8	1694.5
:	:	93		10869.0	10391.4	253.6	251.1		-43.2		43.2			85.1	1716.6
:	:	94		11000.8	10496.7	248.0	246.8		-44.2		43.8			84.0	1732.0
:	38:06	95		11161.3	10663.3	242.6	240.5		-45.4		44.3			82.3	1756.4
:	:	96		11388.0	10805.8	237.2	236.0		-45.2		39.0			80.6	1777.2

Table 4. Flight Data for Flight Number 2, Sonde Number 10

Time GMT H M S	Time To M S	NWS Baro Cont.	NASA Radar ALT-M	NWS ALT-M	MRS ALT-M	NWS Press. mb	MRS Press. mb	NWS Temp. °C	MRS Temp. °C	NWS R.H. %	MRS R.H. %	NWS Refr. Index		MRS Refr. Index	
												N	M	N	M
15:19:45	00:00	3.9	-	4		1024.9		9.4		10.0					
15:20:39	00:54	6.05	-	209		1000.0		10.9		91.7					
15:22:39	02:54	11.0	-	692		944.0		12.6		92.2					
15:25:51	06:06	19.65	-	1568		850.0		8.3		92.3					
15:28:45	09:00	30.3	2675	2691		741.0		1.8		93.4					
15:29:03	09:18	31.0	2758	2756		735.0		-2.2		38.0					
15:29:51	10:06	32.0	2898	2866		725.0		3.8		26.5					
15:31:09	11:24	34.57	3176	3151		700.0		4.3		<10.0					
15:40:39	20:54	57.15	5847	5806		500.0		-12.1		<10.0					
15:42:09	22:24	61.0	6331	6292		469.0		-15.5		22.5					
15:43:27	23:42	64.3	6754	6721		443.0		-18.6		73.2					
15:44:21	24:36	66.0	7029	6942		430.0		-19.4		17.5					
15:46:03	26:18	70.08	7519	7478		400.0		-21.3		15.0					
15:53:03	33:18	85.06	9589	9531		300.0		-37.7		12.5					
15:57:09	37:24	93.64	10813	10762		250.0		-47.7		10.0					
16:01:57	42:12	103.28	12241	12202		200.0		-58.1		10.0					
16:06:33	46:48	112.9	-	13688		157.0		-69.2		10.0					
16:07:21	47:36	114.6	-	13961		150.0		-68.5		10.0					
16:10:39	50:54	120.8	-	14996		126.0		-72.3		10.0					

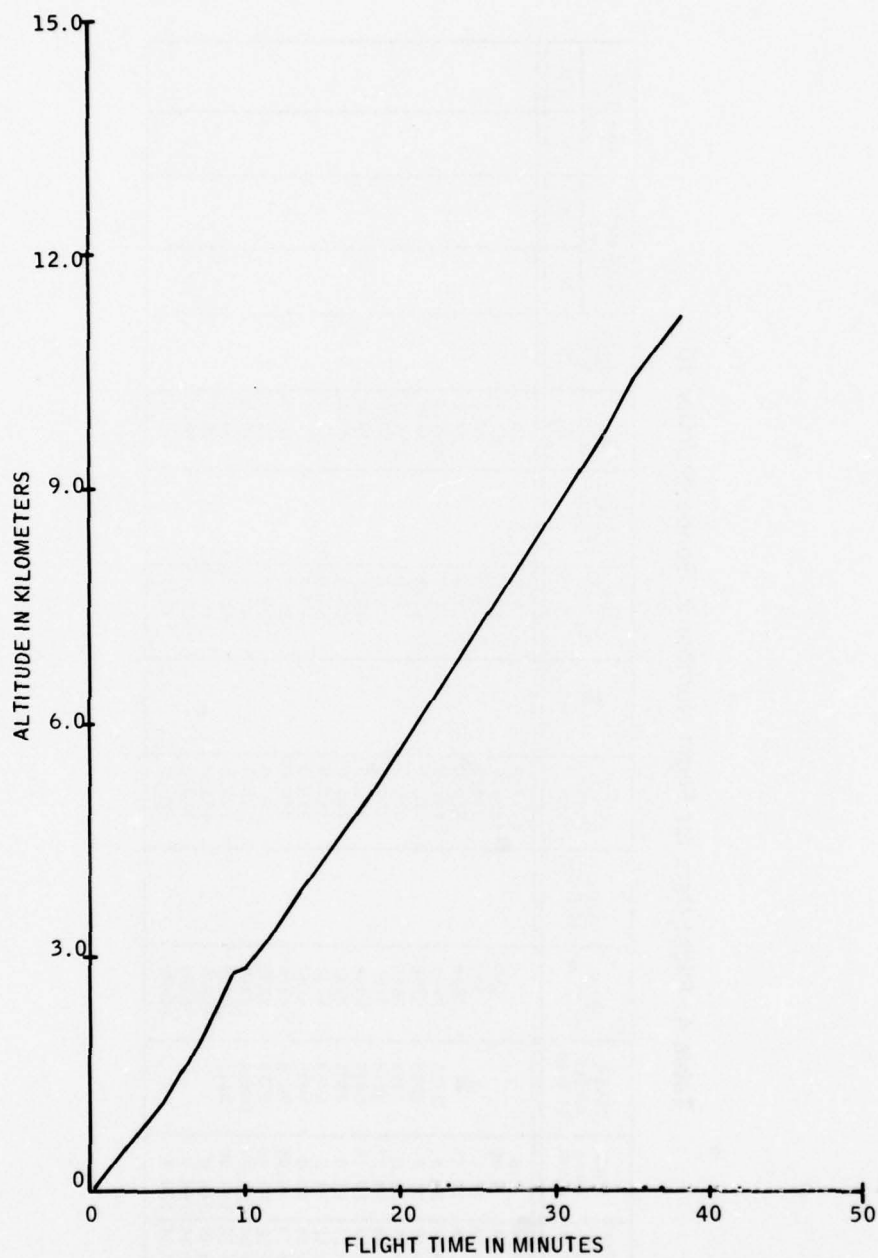


Figure 16. Plot of Altitude versus Time Measured with Mini-Refraction Sonde — Flight Number 2

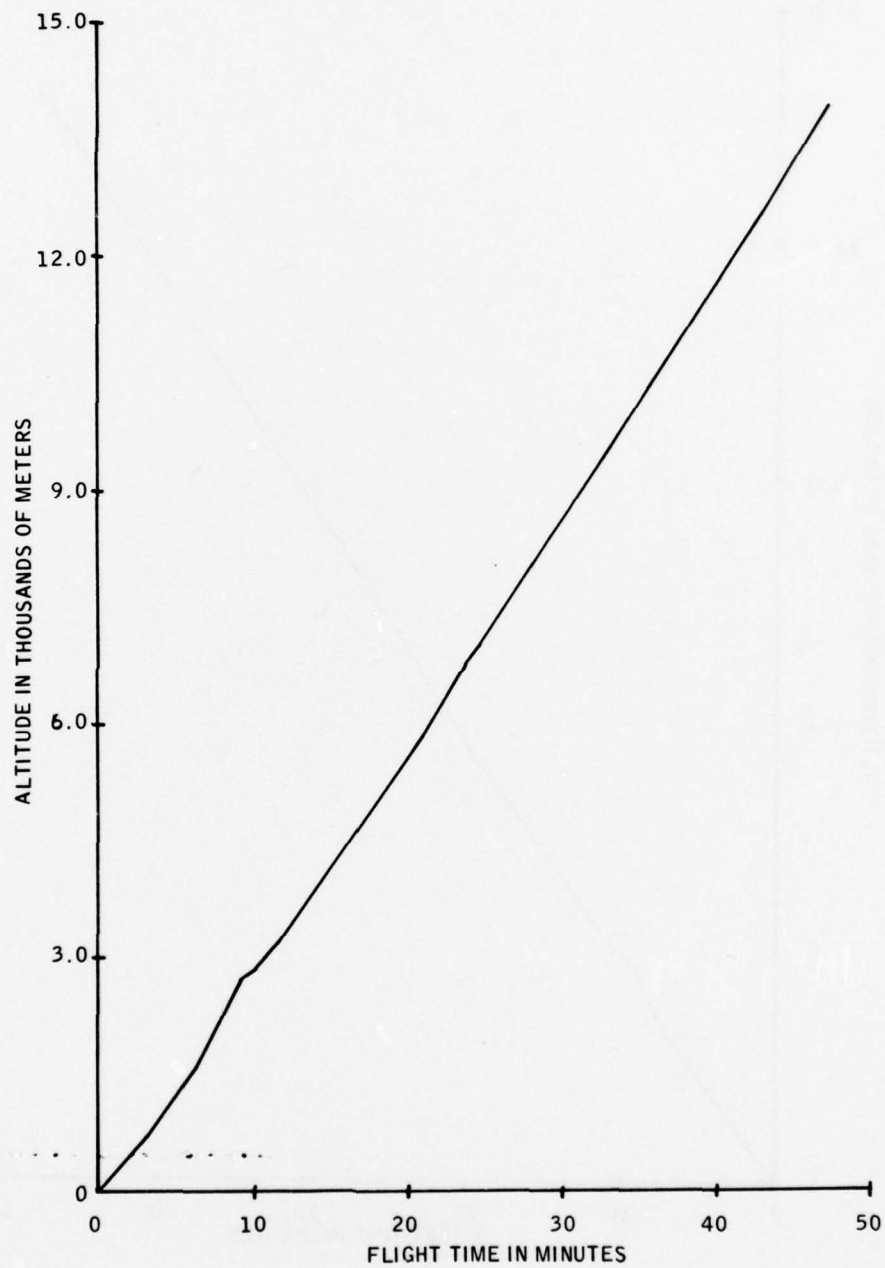


Figure 17. Plot of Altitude versus Time Measured with NWS Rawinsonde — Flight Number 2

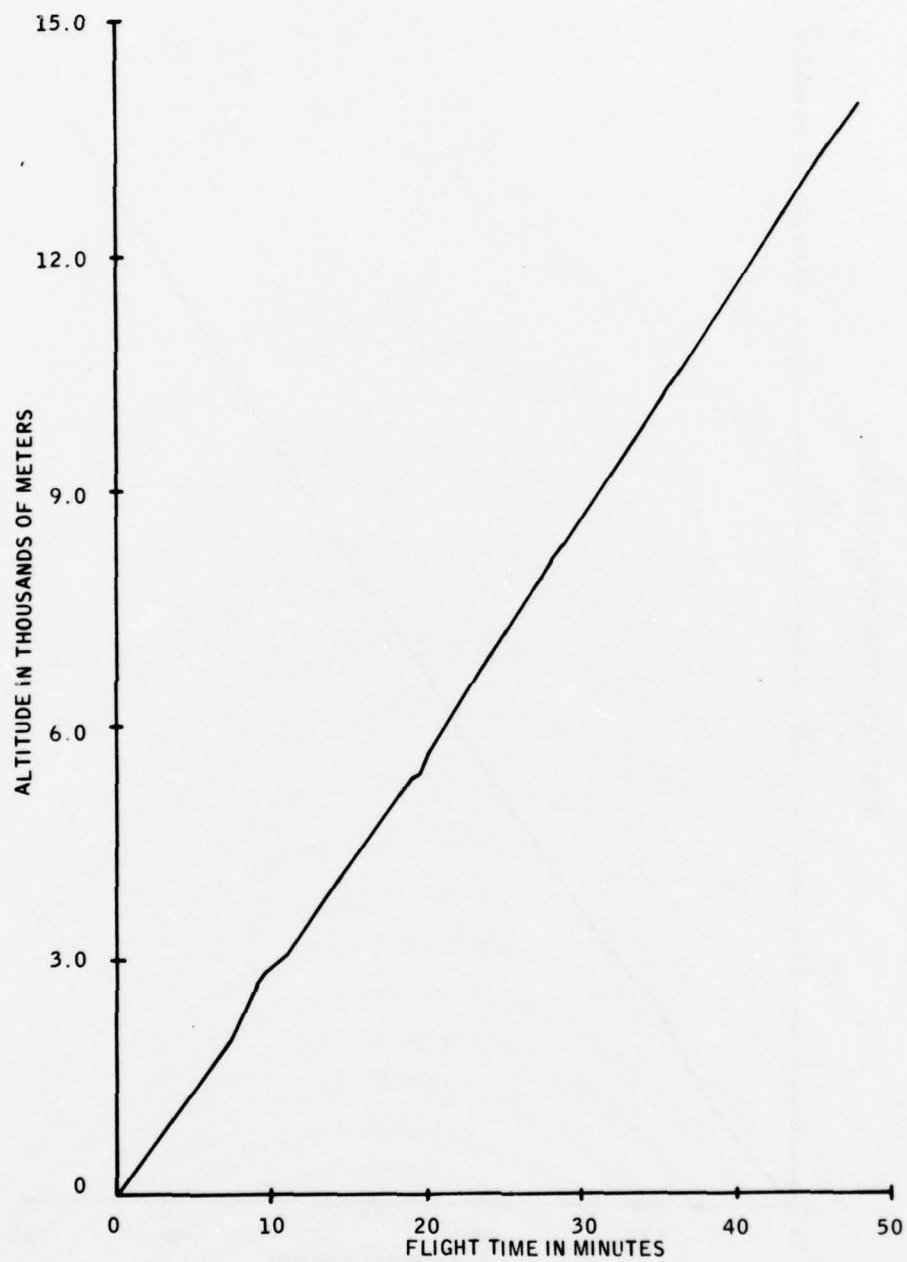


Figure 18. Plot of Altitude versus Time Measured with NASA Radar — Flight Number 2

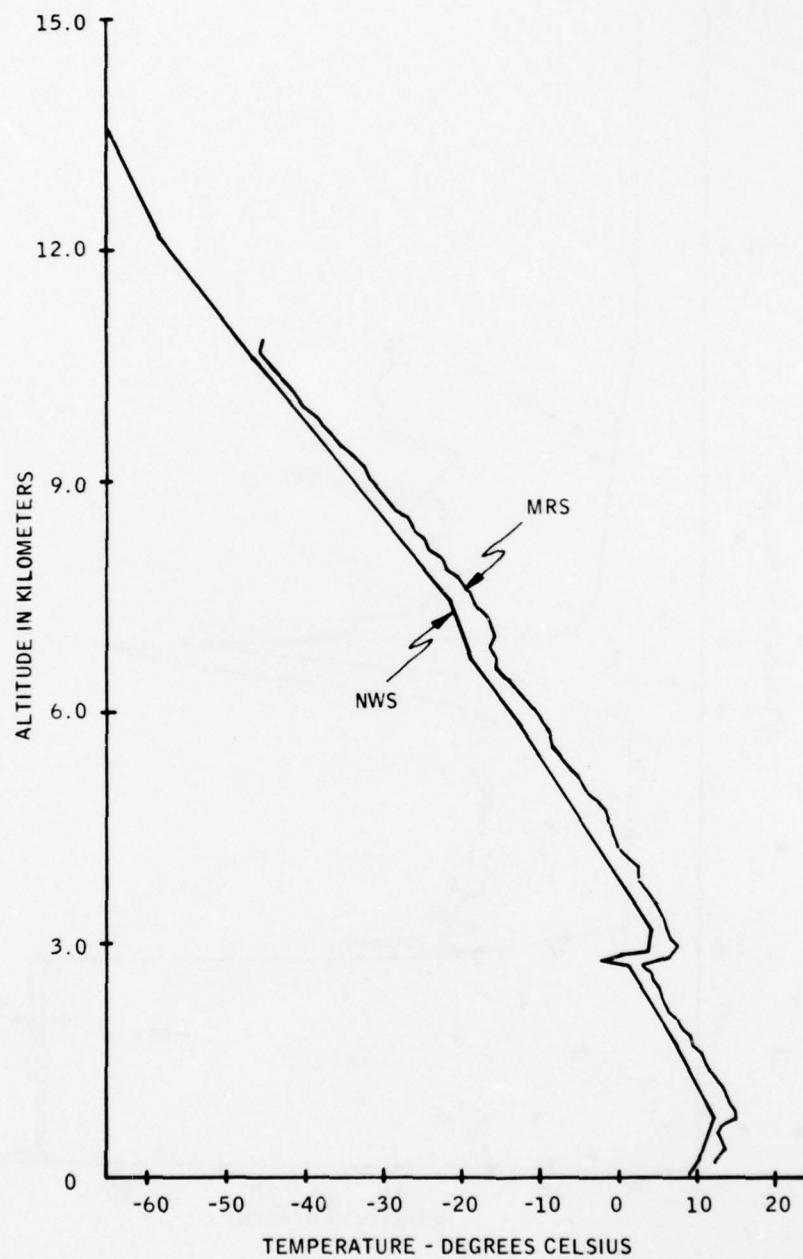


Figure 19. Plot of Free-Air Temperature versus Altitude for the MRS and Rawinsonde — Flight Number 2

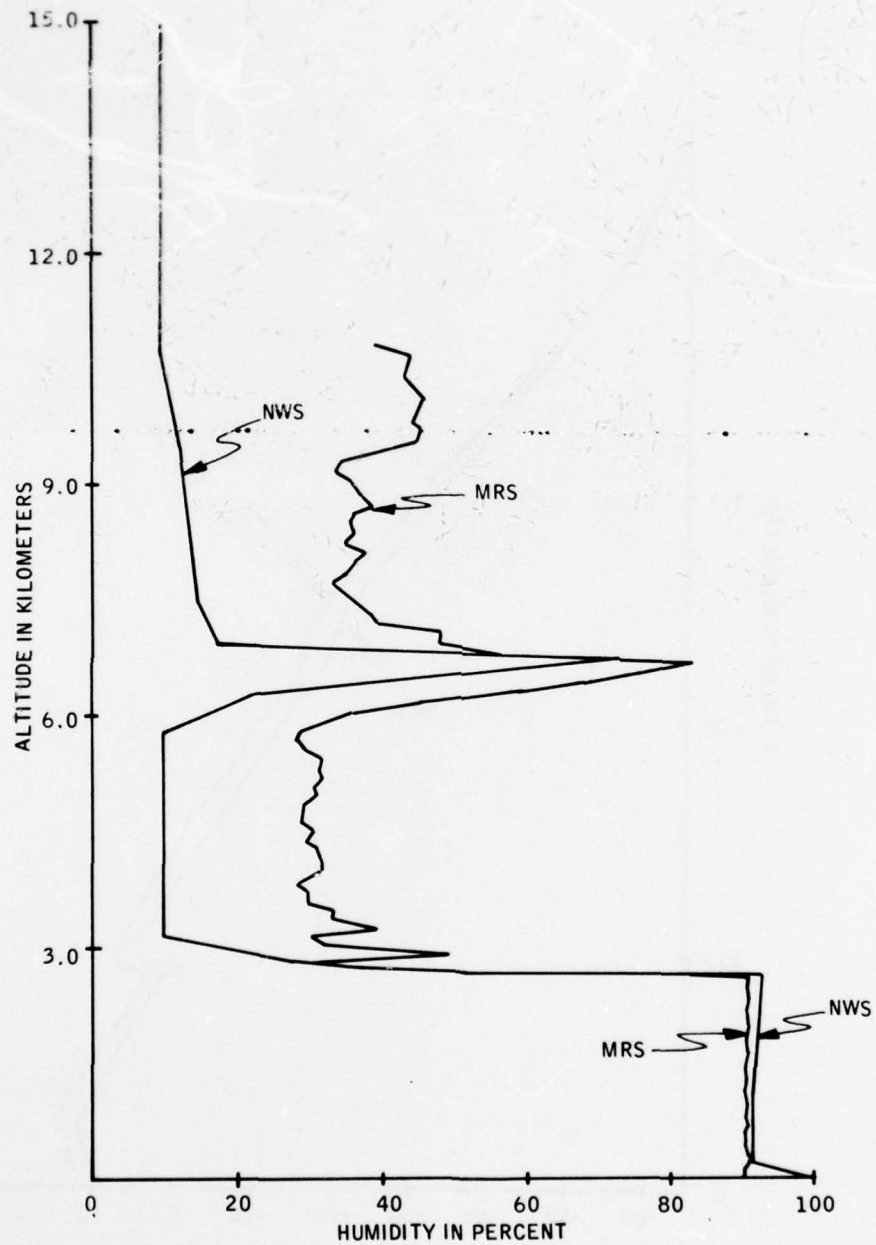


Figure 20. Plot of Relative Humidity versus Altitude for the MRS and Rawinsonde — Flight Number 2

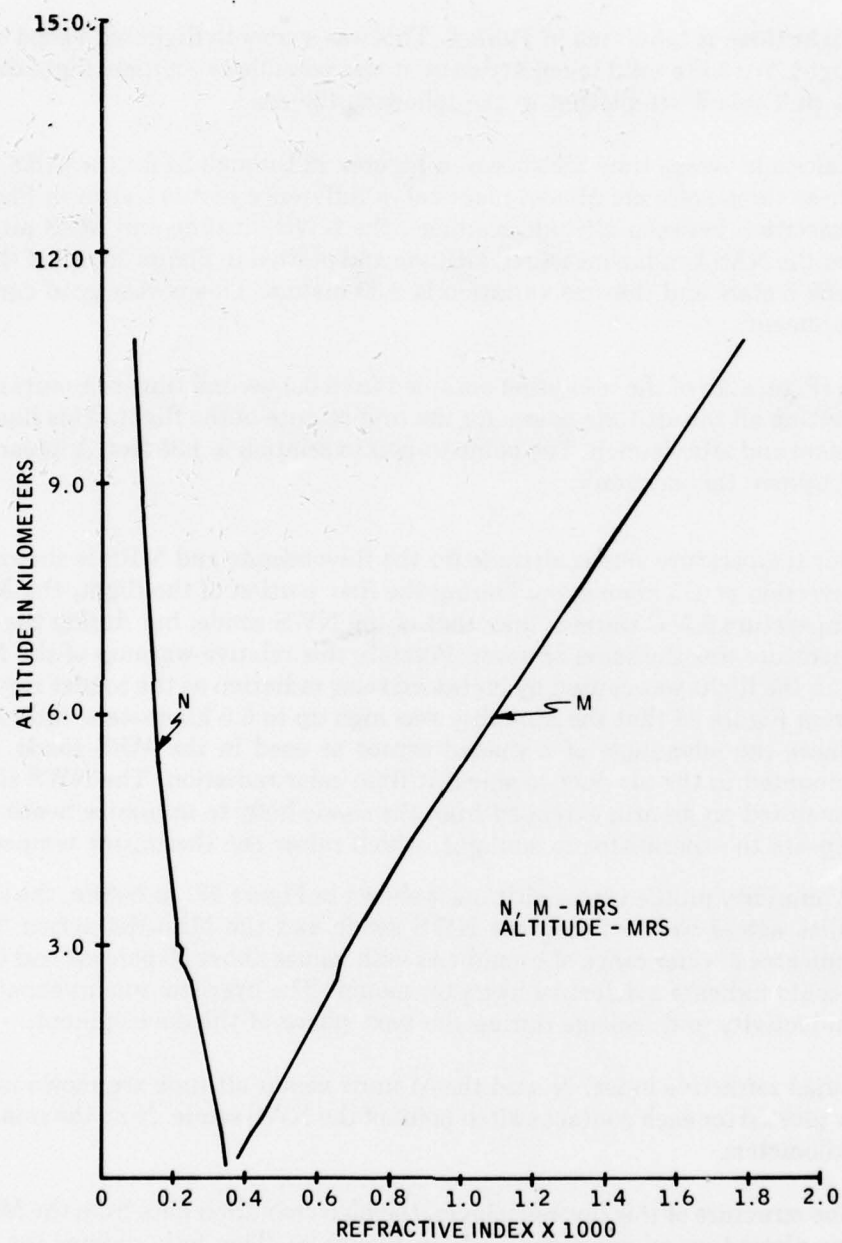


Figure 21. Plot of Modified Refractive Index, N, and M-Units versus Altitude Read by Mini-Refracton Sonde — Flight Number 2

C. FLIGHT NUMBER THREE

The data for flight three is tabulated in Table 5. This was a smooth flight with good data reception over the flight. With the solid telemetry data, it was possible to compare flight data closely. All of the data in Table 5 are plotted in the following figures.

Plots of sonde altitude versus time are shown in Figures 22 through 24 for the MRS, NWS and radar. Since these three plots are almost identical, a difference plot is shown in Figure 25. To illustrate the variation between altitude readings, the NWS altitude and MRS altitude were subtracted from the NASA radar-measured altitude and plotted in Figure 25. All of the readings agree within ± 50 meters and the rms variation is ± 30 meters. This is very good agreement on altitude measurement.

An illustration (Figure 26) of the resolution obtained from 0.4-second time commutation of data is shown by plotting all the altitude points for the first minute of the flight. This illustrates the data scatter before and after launch. The point-to-point variation is ± 35 feet. A linear regression curve fit will improve this accuracy.

A plot of free-air temperature versus altitude for the Rawinsonde and MRS is shown in Figure 27. Note the inversion at 1.5 kilometers. During the first portion of the flight, the MRS sonde indicated a temperature 2.5°C warmer than that of the NWS sonde, but during the rest of the flight the temperature was the same or lower. Possibly this relative warmup of the NWS measurement later in the flight was caused by increased solar radiation as the sondes rose above the clouds. Note from Figure 28 that the humidity was high up to 6.5 kilometers, indicating cloud layers. This shows the advantage of a shaded sensor as used in the MRS sonde. The MRS thermistor is mounted in the air duct to shield it from solar radiation. The NWS Rawinsonde thermistor is mounted on an arm extended from the sonde body to minimize heating from the sonde. This exposes the thermistor to sunlight, which raises the thermistor temperature.

The measured humidity profile versus altitude is shown in Figure 28. As before, the shape of the humidity profiles agrees well between the NWS sonde and the Mini-Refraction Sonde. The NWS sonde indicates a wider range of humidities with values above 90 percent and less than 20 percent. This could indicate a defective hygistor mount. The hygistor mount should be investigated for conductivity and leakage during the next phase of the development.

A plot of modified refractive index, N , and the M-units versus altitude are shown in Figure 29. The values are plotted for each contact switch point of the NWS sonde. Note the small inversion layer at two kilometers.

To show the fine structure of this inversion layer, the high resolution data from the Mini-Refraction Sonde was plotted on an expanded scale in Figure 30. This fully defines the layer.

Table 5. Flight Data for Flight Number 3, Sonde Number 9

Time GMT H M S	Time T o + M S	NWS Baro. Cont.	NASA Radar ALT-M	NWS ALT-M	MRS ALT-M	NWS Press. mb	MRS Press. mb	NWS Temp. °C	MRS Temp. °C	NWS R.H. %	MRS R.H. %	NWS Refr. Index		MRS Refr. Index	
												N	M	N	M
19:07:30	00:06	5			61.3	1015.0	1013.6	11.2	13.7	-	90.2	343.8	353.8	338.4	348.2
19:07:57	00:03	6	-		153.8	1001.8	1002.8	12.5	14.3	97.7	91.2	342.7	366.8	338.0	361.7
19:08:21	00:57	7	-		266.7	990.2	990.0	12.8	14.6	97.8	91.3	340.3	381.4	335.4	375.8
19:08:45	01:21	8	-		380.4	977.4	977.7	12.5	14.5	97.7	91.4	336.8	393.4	331.9	388.5
19:09:09	01:45	9	-		467.7	966.0	966.3	13.0	14.9	97.8	91.4	335.2	408.8	330.2	402.0
19:09:36	02:12	10	-		563.2	954.4	954.8	13.0	14.9	-	91.4	331.7	420.8	327.0	414.3
19:10:00	02:36	11	-	670	664.9	943.2	943.3	13.2	15.0	97.5	91.5	328.8	434.0	324.2	427.3
19:10:24	03:00	12	-		777.9	932.0	932.0	13.2	14.9	97.5	91.5	326.1	447.3	321.1	439.8
19:10:48	03:24	13	-		874.7	920.6	920.9	12.8	14.8	97.8	91.6	322.0	458.9	317.6	451.8
19:11:09	03:45	14	-		973.5	909.6	910.4	12.0	14.2	97.9	91.4	317.2	469.1	312.9	461.9
19:11:33	04:09	15	-		1070.9	898.4	898.4	11.3	13.4	-	91.1	311.0	480.3	307.0	472.9
19:11:57	04:33	16	-		1185.0	887.2	887.5	10.4	12.8	96.0	90.8	305.6	490.8	302.1	483.6
19:12:21	04:57	17	-		1290.7	876.2	876.8	9.5	12.2	94.8	89.0	300.2	501.1	296.5	493.5
19:12:42	05:18	18	-		1393.9	865.0	865.7	9.2	11.4	95.0	89.8	295.4	512.8	292.1	505.1
19:13:06	05:42	19	-		1502.2	854.0	854.9	8.3	10.8	97.5	89.8	292.1	525.7	287.6	516.5
19:13:30	06:06	20	1604		1581.7	843.6	844.5	7.5	10.0	-	89.9	280.5	529.8	283.0	527.3
19:13:54	06:30	21	1719		1703.9	833.0	833.9	6.2	9.7	73.5	74.9	270.0	535.5	270.8	531.1
19:14:15	06:51	22	1821		1802.9	822.2	823.2	5.9	9.5	63.0	68.3	260.8	543.0	263.9	540.6
19:14:39	07:15	23	1933		1937.7	811.8	811.9	6.2	10.3	36.0	49.0	243.2	543.8	250.8	545.7
19:15:00	07:36	24	2014		2009.9	801.4	802.4	7.6	10.8	37.0	45.6	241.3	558.3	246.7	556.9
19:15:24	08:00	25	2130	2128	2138.4	791.0	792.1	8.3	10.7	-	63.9	256.7	590.1	254.6	581.6
19:15:48	08:24	26	2236	2233	2246.1	780.8	781.9	8.5	10.8	97.5	92.6	272.1	623.1	269.3	613.2
19:16:15	08:51	27	2353		2347.4	770.6	771.6	7.9	10.3	98.3	93.5	268.4	636.4	265.8	626.6
19:16:39	09:15	28	2452		2458.4	760.4	762.0	7.6	10.1	97.3	92.8	264.4	648.7	262.2	638.8
19:17:03	09:39	29	2568		2572.5	750.4	751.9	7.0	9.5	96.3	92.2	259.8	661.2	257.6	650.9
19:17:27	10:03	30	2690		2668.6	740.6	742.1	6.5	8.7	-	92.9	255.5	673.5	253.5	663.2
19:17:51	10:27	31	2797		2804.0	730.8	732.0	5.7	8.2	97.0	93.0	251.6	687.0	249.7	676.4
19:18:18	10:54	32	2921		2929.3	720.8	722.8	5.0	7.7	97.2	93.0	247.4	700.1	246.0	688.6
19:18:45	11:21	33	3055		3037.0	711.0	711.2	4.2	7.0	96.9	92.8	243.1	715.2	241.3	704.0
19:19:06	11:42	34	3163		3153.4	701.2	701.2	3.7	6.2	88.7	88.1	235.0	724.6	234.8	714.8
19:19:30	12:06	35	3283		3276.9	691.6	691.0	3.2	5.6	-	86.9	231.0	739.1	230.4	728.5
19:19:57	12:33	36	3410		3375.0	682.2	682.3	2.3	5.1	88.3	86.9	227.5	751.5	227.0	740.8
19:20:21	12:57	37	3512		3493.6	673.0	672.4	1.6	4.2	95.6	85.9	188.3	729.4	222.6	754.0
19:20:45	13:21	38	3624		3608.7	663.4	662.3	0.8	3.7	97.8	93.7	223.7	785.2	222.0	772.3

Table 5. Flight Data for Flight Number 3, Sonde Number 9 (Continued)

Time GMT	Time T + M S	NWS Baro. Cont.	NASA Radar ALT-M	NWS ALT-M	MRS ALT-M	NWS Press. mb	MRS Press. mb	NWS Temp. °C	MRS Temp. °C	NWS R.H. %	MRS R.H. %	NWS Refr. Index		MRS Refr. Index	
												N	M	N	M
19-21:09	13:45	39	3733		3727.1	654.2	653.4	0.2	3.1	96.5	92.7	219.5	797.8	218.2	784.9
19-21:33	14:09	40	3828		3831.4	645.2	644.6	0	2.7	-	83.9	214.7	811.2	211.9	795.3
19-22:00	14:36	41	3949		3957.0	635.8	635.1	-0.6	2.0	87.9	86.1	210.0	822.4	209.1	810.4
19-22:24	15:00	42	4068		4074.0	626.6	626.0	-1.6	1.1	95.1	89.8	208.3	839.7	206.5	825.2
19-22:48	15:24	43	4180		4192.8	617.8	617.2	-2.4	0.5	97.5	93.2	205.7	854.7	204.4	840.4
19-23:15	15:51	44	4295		4309.0	609.0	610.1	-3.4	-0.3	96.8	93.0	201.8	869.3	201.4	850.9
19-23:39	16:15	45	4399		4431.2	600.0	599.4	-4.0	-0.9	-	92.3	197.1	881.7	197.3	868.4
19-24:06	16:42	46	4531	4484	4540.4	591.2	590.6	-4.7	-1.6	86.8	87.9	192.5	895.1	192.9	881.5
19-24:33	17:09	47	4658		4660.6	581.4	581.3	-5.0	-2.4	50.0	62.2	179.6	901.4	182.8	890.1
19-24:57	17:33	48	4766		4772.6	573.0	572.9	-5.7	-2.9	83.8	78.4	185.6	925.4	184.2	909.2
19-25:21	17:57	49	4871		4894.1	564.4	564.4	-6.7	-3.6	92.0	90.8	184.6	942.8	184.3	927.1
19-25:51	18:27	50	5010		5026.7	556.0	556.3	-7.0	-4.0	-	94.3	182.6	959.4	182.4	943.0
19-26:15	18:51	51	5126		5137.9	547.6	547.6	-7.6	-4.8	98.9	94.5	180.2	975.4	179.2	958.3
19-26:42	19:18	52	5250		5252.0	539.4	539.3	-8.3	-5.4	99.4	94.5	177.4	991.1	176.4	973.7
19-27:03	19:39	53	5345		5378.2	531.0	531.0	-8.7	-6.2	99.8	94.6	174.4	1006.6	173.4	988.7
19-27:30	20:06	54	5490		5507.0	523.0	523.1	-9.3	-6.6	99.0	94.5	171.5	1022.0	170.8	1004.1
19-27:57	20:33	55	5595		5625.7	515.0	515.2	-10.0	-7.5	-	94.3	168.5	1037.0	167.8	1018.8
19-28:21	20:57	56	5714		5738.4	506.8	506.9	-10.7	-8.3	96.9	94.2	165.3	1053.3	164.9	1034.8
19-28:48	21:24	57	5846		5862.1	499.0	499.2	-11.4	-8.8	94.4	93.7	162.3	1068.4	162.3	1050.1
19-29:15	21:51	58	5970	6049	5978.8	491.2	491.0	-11.7	-8.8	81.8	80.6	158.0	1084.3	157.6	1065.9
19-29:42	22:18	59	6099		6105.5	483.4	483.7	-12.7	-9.6	82.3	80.6	155.4	1100.1	155.2	1080.5
19-30:06	22:42	60	6223		6232.6	475.6	476.4	-13.5	-10.4	-	82.9	149.0	1110.8	153.1	1095.8
19-30:30	23:06	61	6339	6305	6354.6	467.2	468.5	-14.1	-9.6	29.0	45.4	142.5	1127.0	145.1	1109.7
19-30:54	23:30	62	6466		6471.4	460.2	461.5	-14.9	-10.3	17.5	36.5	138.9	1140.7	141.7	1123.7
19-31:21	23:57	63	6601		6574.6	453.0	454.1	-15.8	-11.2	15.0	34.7	136.6	1157.2	139.4	1139.5
19-31:42	24:18	64	6697		6704.8	445.6	447.0	-16.7	-11.9	13.0	32.0	134.5	1173.6	137.0	1155.4
19-32:09	24:45	65	6831		6854.1	437.4	439.3	-17.4	-12.0	-	31.0	132.6	1191.7	134.8	1172.5
19-32:36	25:12	66	6990		6973.6	430.2	431.9	-18.3	-13.8	12.5	30.9	130.7	1209.1	132.8	1189.4
19-33:00	25:36	67	7111		7101.4	423.2	424.9	-19.0	-14.8	11.0	28.2	128.9	1225.5	130.7	1205.2
19-33:27	26:03	68	7233		7219.1	416.0	417.9	-19.8	-15.6	10.0	26.0	127.0	1242.7	128.6	1221.9
19-33:51	26:27	69	7367		7355.3	409.0	411.0	-20.2	-16.7	11.5	26.1	125.4	1260.3	127.0	1238.6
19-34:18	26:54	70	7494		7449.1	402.0	404.6	-21.5	-17.7	-	26.7	123.8	1276.4	125.2	1253.7
19-34:48	27:24	71	7626		7601.0	395.2	397.5	-22.5	-18.6	10.0	29.3	122.0	1294.0	123.5	1271.7
19-35:15	27:51	72	7742		7732.8	388.4	390.6	-23.4	-19.6	10.2	26.5	120.3	1311.7	121.5	1286.8

Table 5. Flight Data for Flight Number 3, Sonde Number 9 (Concluded)

Time GMT H M S	Time To + M S	NWS Baro. Cont.	NASA Radar ALT-M	NWS ALT-M	MRS ALT-M	NWS Press. mb	MRS Press. mb	NWS Temp. °C	MRS Temp. °C	NWS R.H. %	MRS R.H. %	NWS Refr. Index		MRS Refr. Index	
												N	M	N	M
19:35:45	28:21	73	7882		7847.0	381.8	383.5	-24.4	-20.6	10.3	26.6	118.6	1329.9	119.7	1307.0
19:36:12	28:48	74	8000		7978.7	375.2	377.5	-25.5	-21.4	10.1	26.4	117.0	1346.8	118.1	1322.5
19:36:39	29:15	75	8106		8102.8	368.4	371.0	-26.5	-22.8	--	26.8	115.6	1363.8	116.6	1338.7
19:37:09	29:45	76	8263		8260.2	362.0	364.1	-27.6	-23.5	12.0	27.5	114.3	1384.0	114.7	1357.9
19:37:33	30:09	77	8381		8373.5	355.4	358.0	-28.5	-24.9	12.0	27.4	112.5	1398.5	113.3	1373.3
19:38:00	30:36	78	8520		8514.4	349.0	351.5	-29.5	-25.8	10.0	26.3	110.8	1416.8	111.5	1391.5
19:38:27	31:03	79	8655		8624.6	342.8	345.4	-30.5	-26.8	10.1	25.3	109.2	1435.2	109.9	1408.3
19:38:51	31:27	80	8769		8726.8	336.6	339.5	-31.5	-27.7	--	25.5	107.8	1452.6	108.3	1425.1
19:39:18	31:54	81	8899		8892.3	330.4	333.0	-32.6	-29.0	11.0	26.4	106.2	1471.3	106.7	1443.4
19:39:45	32:21	82	9052		9015.4	324.4	327.0	-33.6	-30.3	12.5	28.5	104.9	1488.6	105.4	1460.4
19:40:09	32:45	83	9180		9151.4	318.4	321.7	-34.6	-31.3	13.0	29.3	103.6	1504.9	104.1	1475.6
19:40:36	33:12	84	9296		9283.9	312.4	315.4	-35.7	-32.5	15.0	31.5	102.1	1524.1	102.5	1494.4
19:41:00	33:36	85	9438		9398.2	306.6	309.7	-36.7	-32.9	--	32.0	100.4	1543.5	100.8	1513.0
19:41:24	34:00	86	9567		9548.9	300.8	303.7	-37.8	-34.8	15.0	32.4	99.2	1559.8	99.6	1529.8
19:41:51	34:27	87	9700		9665.8	295.0	298.3	-38.7	-35.4	15.1	32.3	97.6	1578.8	98.0	1547.8
19:42:18	34:54	88	9833		9786.0	289.4	292.6	-40.0	-36.6	18.0	34.8	96.4	1596.0	96.6	1565.5
19:42:42	35:18	89	9957		9928.6	283.6	287.3	-41.0	-37.7	24.0	37.6	95.1	1614.9	95.3	1582.7
19:43:15	35:51	90	10108		10066.1	278.0	281.8	-42.6	-38.6	--	42.6	93.8	1633.0	93.8	1601.2
19:43:48	36:24	91	10230		10199.0	272.4	276.1	-43.5	-39.8	39.0	45.4	92.3	1653.5	92.4	1620.2
19:44:15	36:51	92	10348		10324.1	267.2	271.1	-44.7	-40.8	47.5	50.1	91.1	1671.1	91.2	1636.8
19:44:48	37:24	93	10495		10457.4	261.8	265.9	-45.5	-42.0	42.0	48.3	89.8	1688.3	89.8	1654.5
19:45:15	37:51	94	10607		10602.7	256.6	260.6	-46.5	-43.2	36.0	45.1	88.3	1707.4	88.4	1672.5
19:45:48	38:24	95	10744		10739.1	251.4	255.2	-47.8	-43.6	--	43.3	86.5	1729.5	86.6	1694.1
19:46:18	38:54	96	10871		10860.9	246.2	250.6	-48.3	-45.2	28.0	40.8	85.5	1745.3	85.6	1709.0
19:46:51	39:27	97	11018		11007.9	241.0	245.1	-48.6	-45.4	18.0	37.2	83.6	1768.5	83.8	1731.8
19:47:18	39:54	98	11163	11119	11141.8	236.0	240.3	-49.8	-46.0	16.5	33.6	82.2	1788.5	82.3	1751.6
19:47:45	40:21	99	11282		11255.5	231.0	235.9	-51.0	-47.3	16.0	32.7	81.2	1804.2	81.3	1767.1
19:48:12	40:48	100	11394		11387.8	226.2	231.3	-52.3	-48.3	--	32.5	79.9	1823.0	80.0	1785.2
19:48:45	41:21	101	11562		11534.8	221.2	226.2	-53.2	-49.2	15.0	32.2	78.4	1844.9	78.5	1806.4
19:49:12	41:48	102	11708		11676.3	216.6	221.7	-54.5	-50.6	15.5	31.3	77.4	1862.1	77.4	1823.3
19:49:39	42:15	103	11857		11798.9	212.0	217.4	-55.7	-51.8	17.5	33.5	76.3	1879.7	76.3	1840.4
19:50:06	42:42	104	11974		11944.0	207.2	212.6	-56.8	-53.4	18.0	34.7	75.1	1899.4	75.2	1859.2
19:50:36	43:12	105	12093		12083.6	202.6	208.2	-57.9	-54.3	--	35.4	73.9	1918.5	74.0	1877.6
19:51:03	43:39	106	12210		12207.5	198.2	204.0	-59.0	-55.4	21.0	35.8	72.8	1937.0	72.8	1895.9

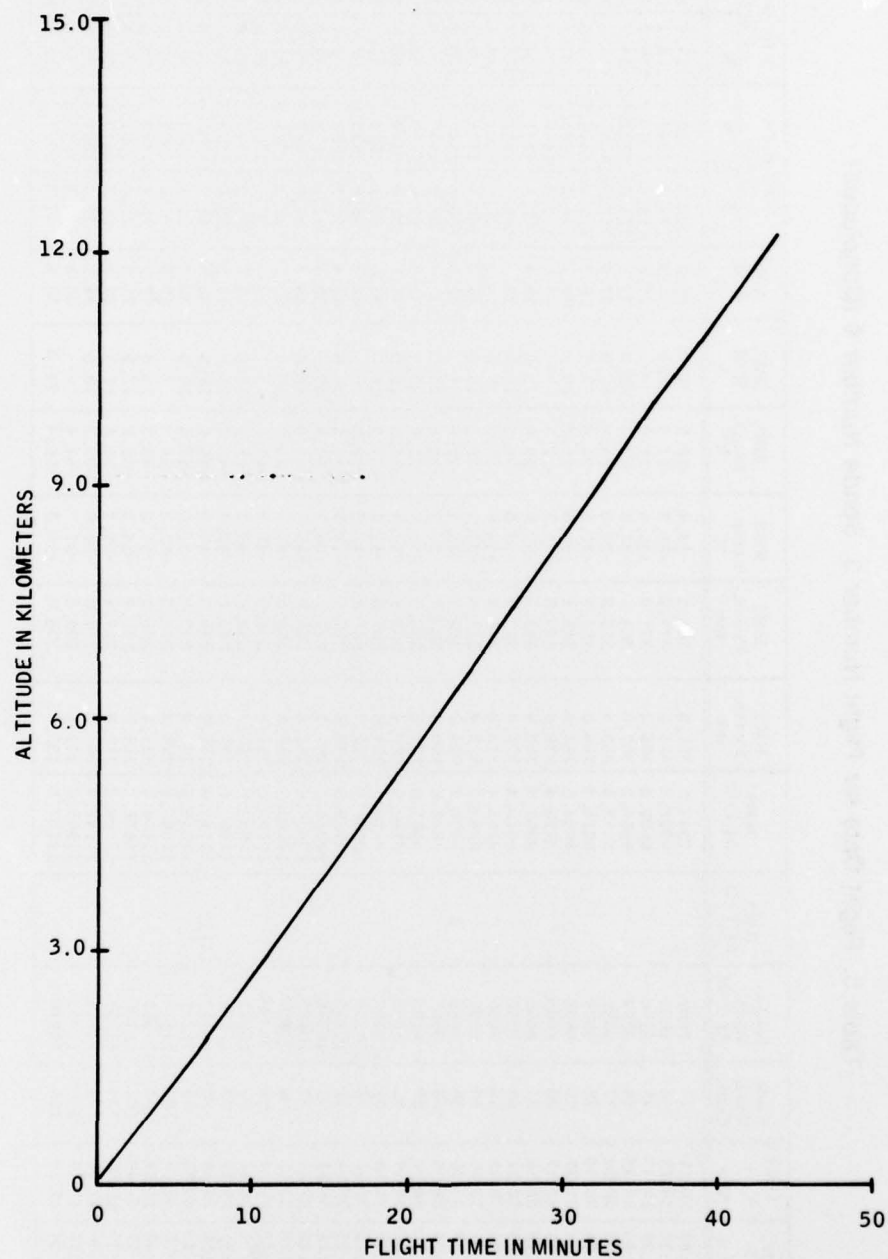


Figure 22. Plot of Altitude versus Time Measured with Mini-Refraction Sonde — Flight Number 3

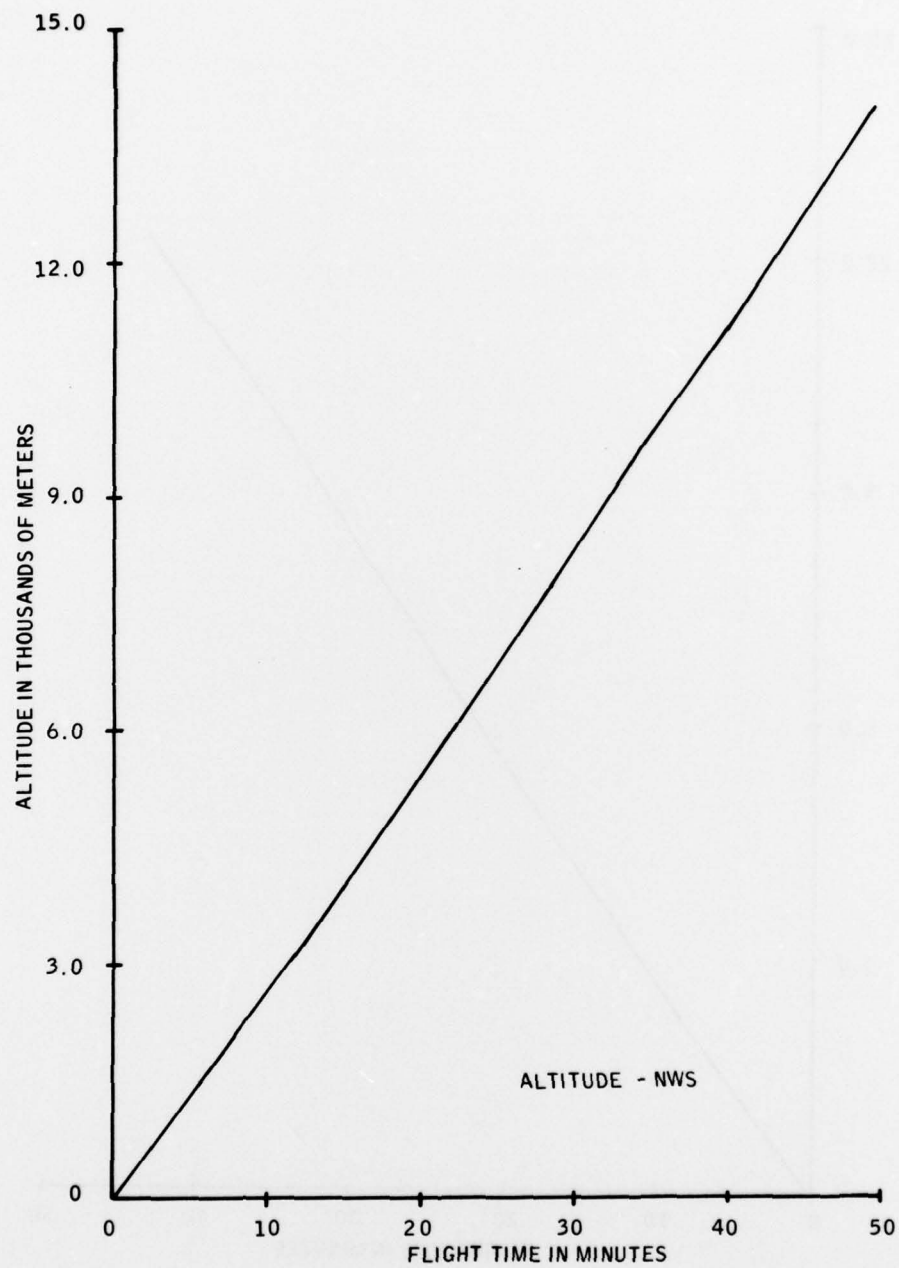


Figure 23. Plot of Altitude versus time Measured with NWS Rawinsonde — Flight Number 3

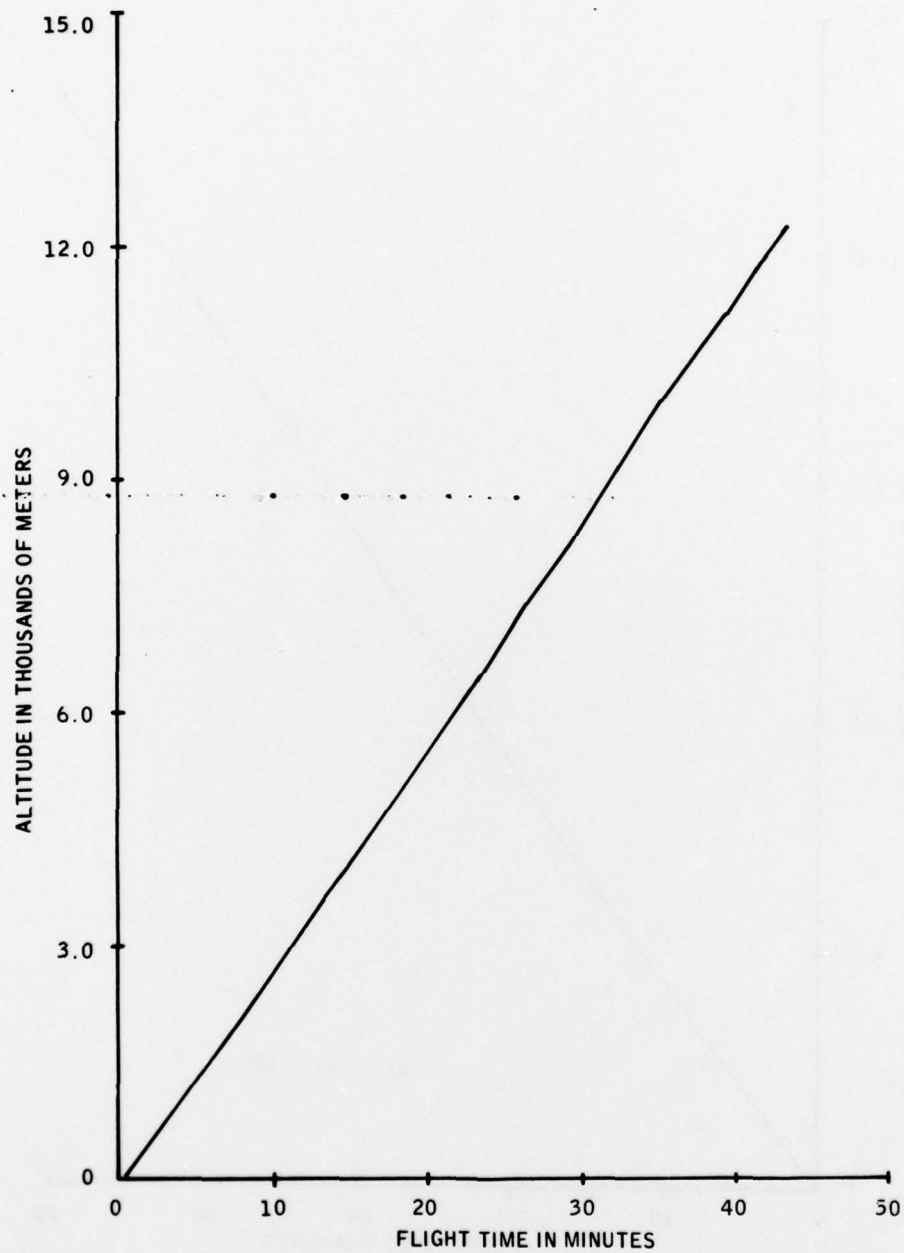


Figure 24. Plot of Altitude versus Time Measured with NASA Radar — Flight Number 3

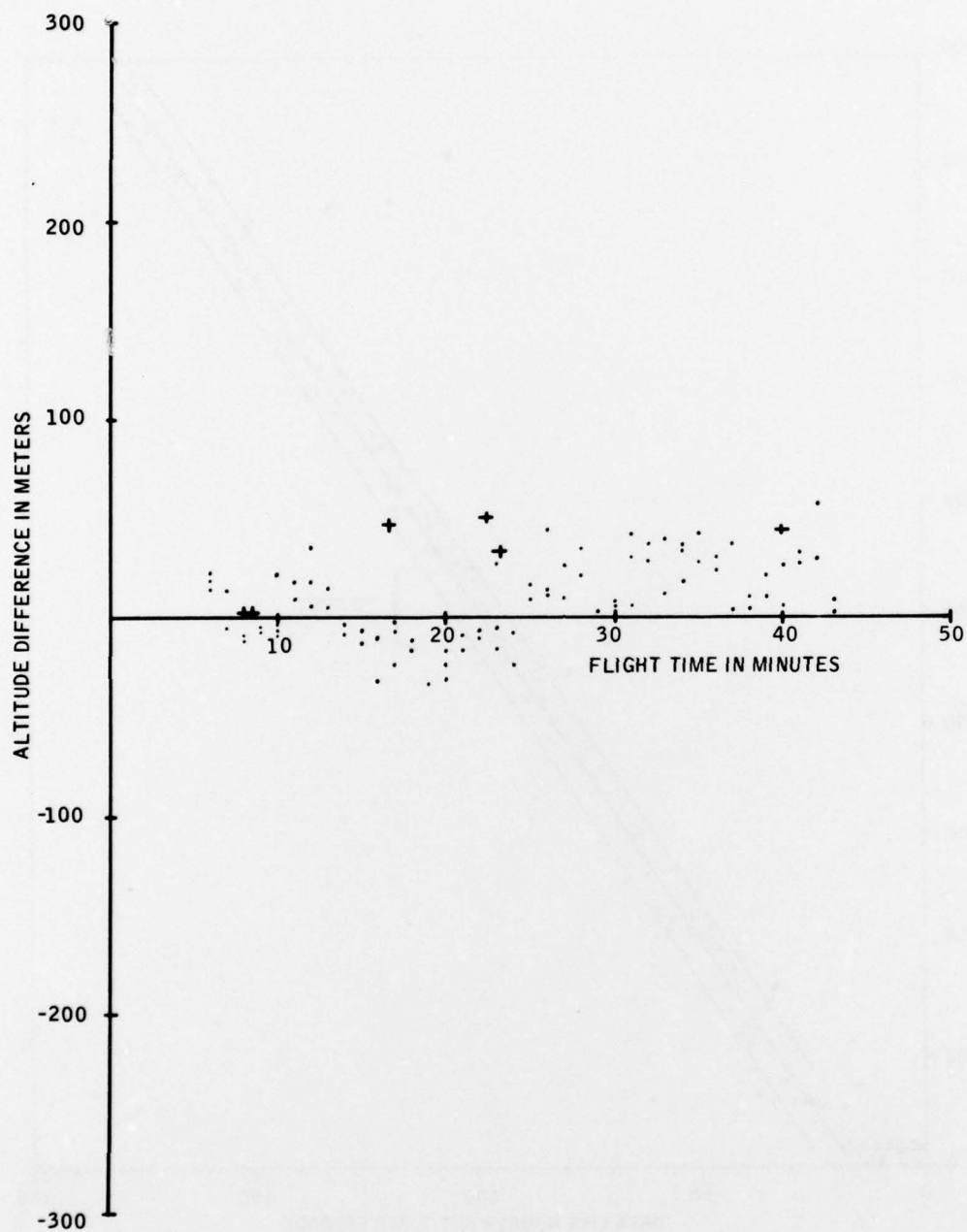


Figure 25. Plot of Difference in Altitude Reading of the MRS and Rawinsonde versus Radar — Flight Number 3

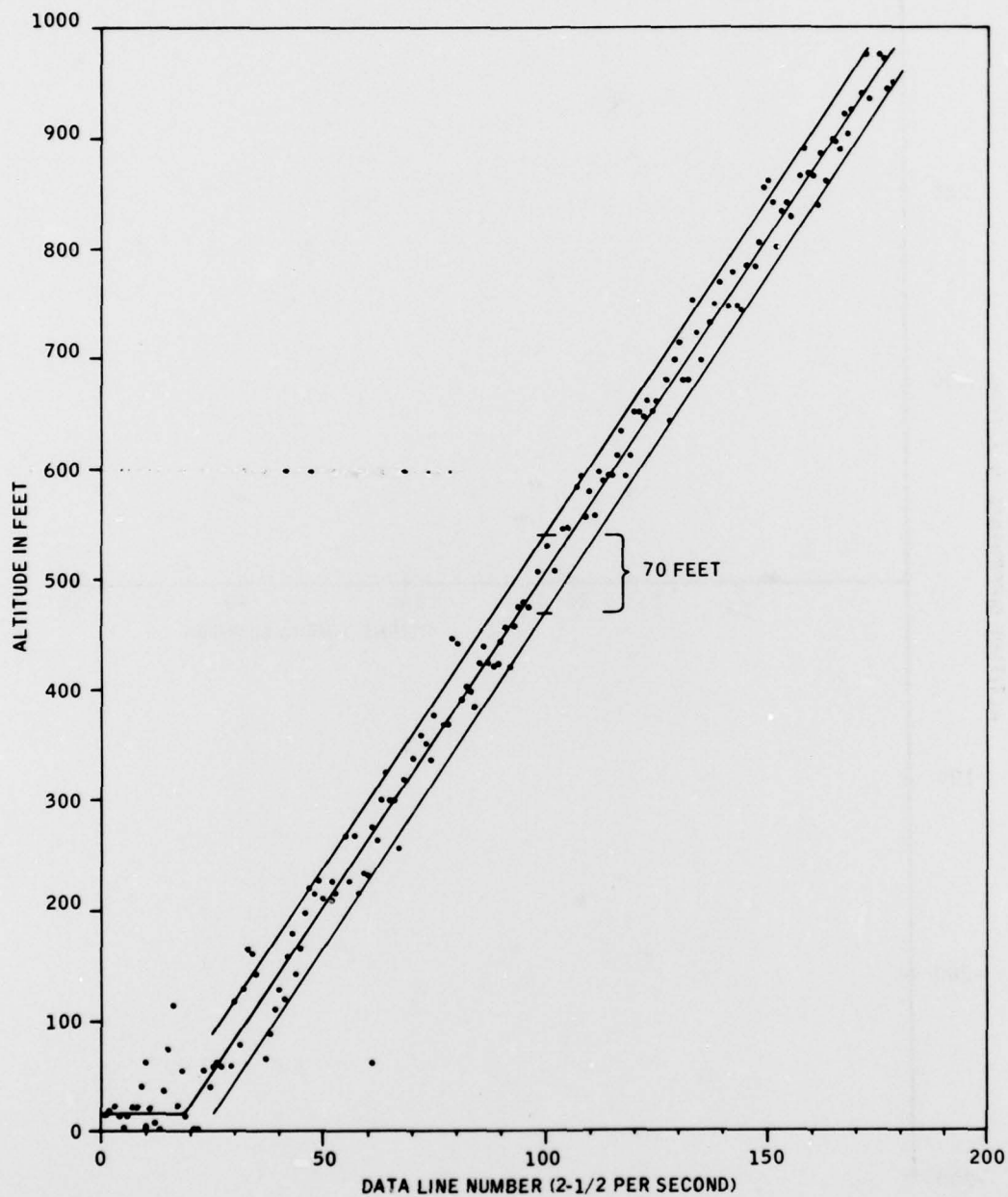


Figure 26. Plot of Altitude versus Time for Flight Number 3 Measured with MRS. Each data point at 2-1/2 per second is plotted to show resolution.

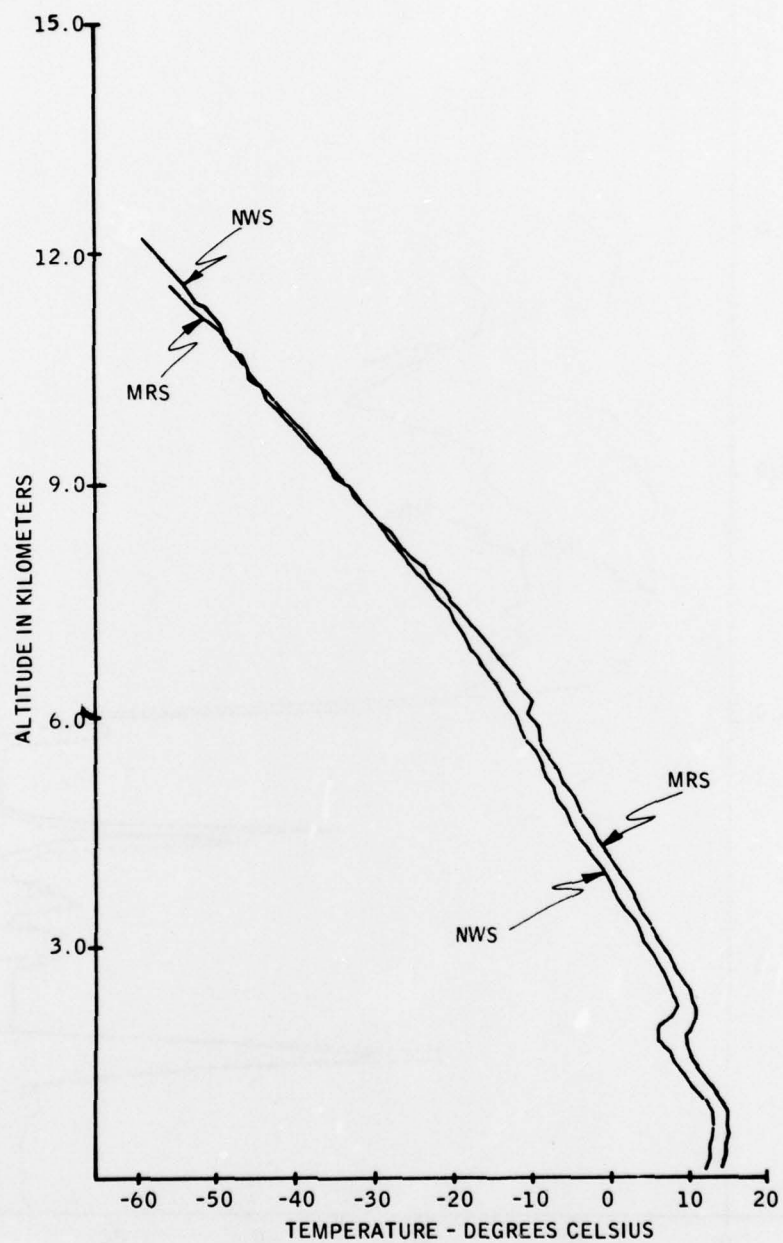


Figure 27. Plot of Free-Air Temperature versus Altitude for the MRS and Rawinsonde — Flight Number 3

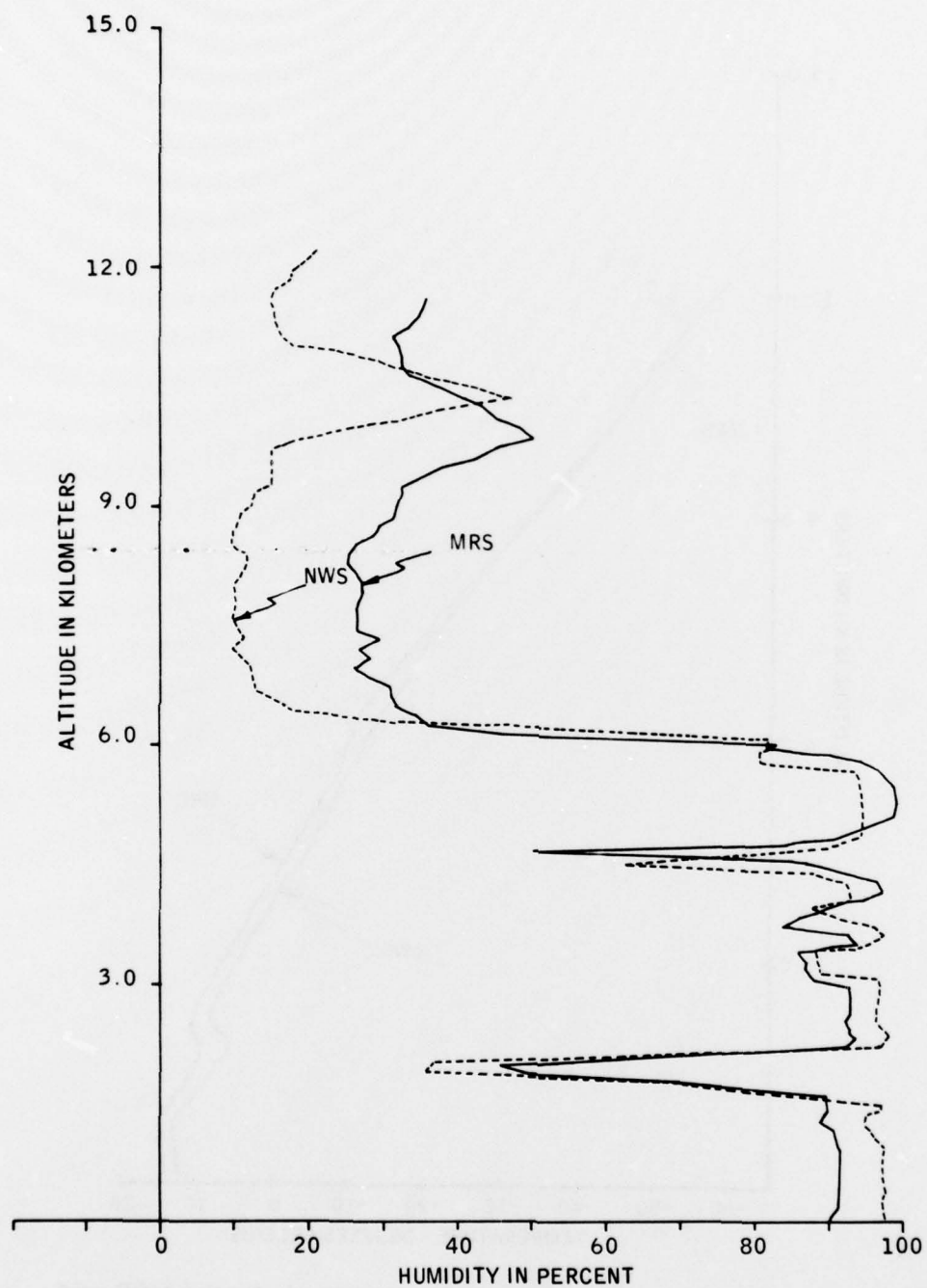


Figure 28. Plot of Relative Humidity versus Altitude for the MRS and Rawinsonde — Flight Number 3

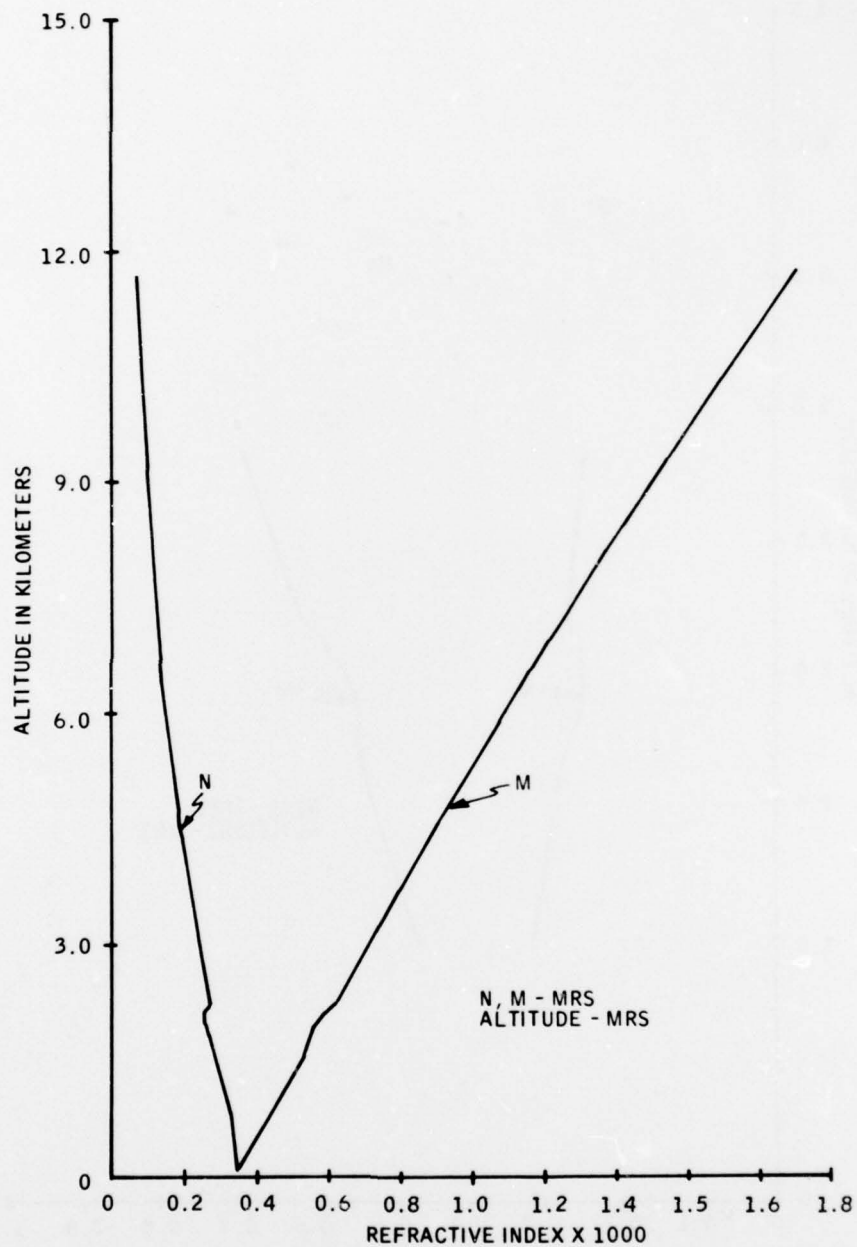


Figure 29. Plot of Modified Refractive Index, N, and M-Units versus Altitude Read by Mini-Refraction Sonde — Flight Number 3

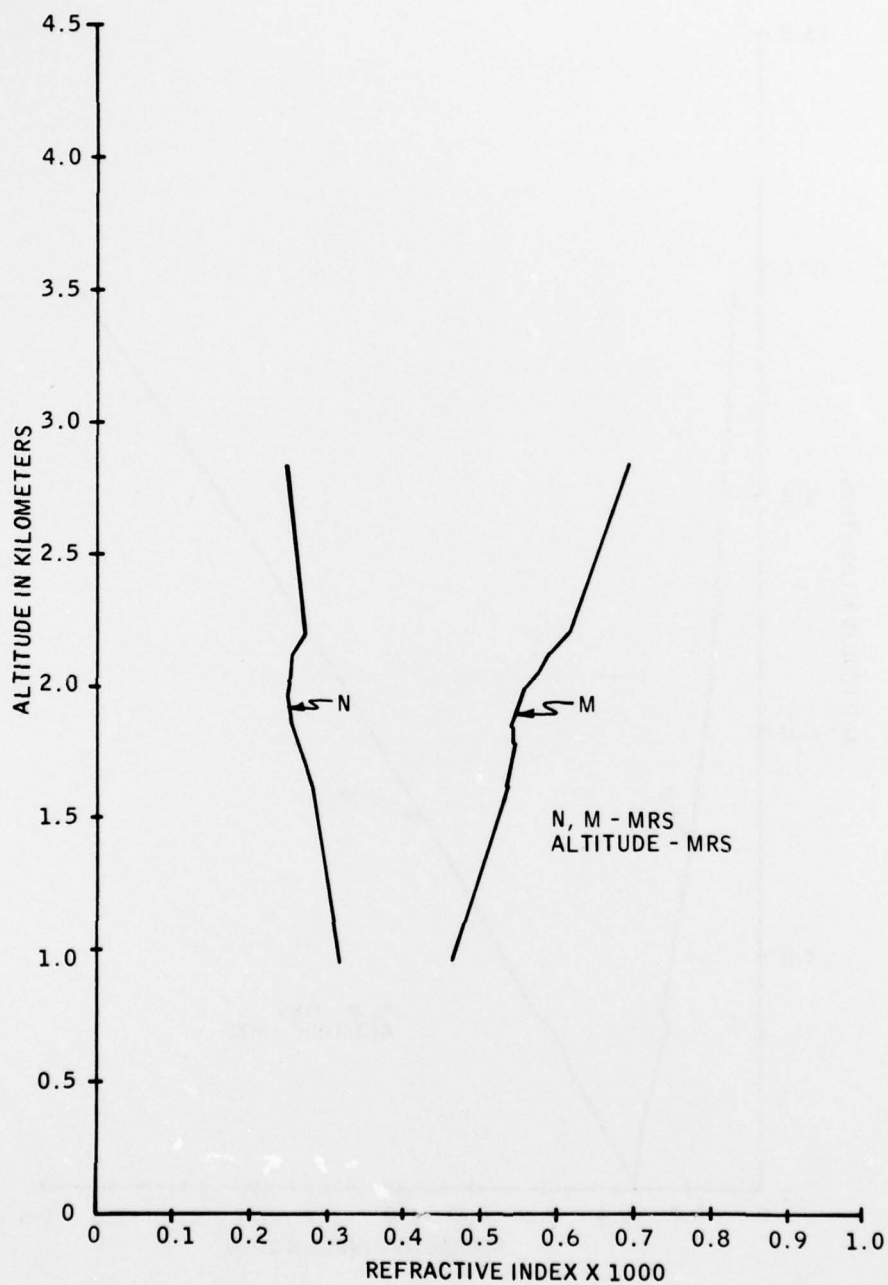


Figure 30. Plot of N and M versus Altitude with an Expanded Scale to Illustrate Resolution

D. DATA REDUCTION

The Mini-Refraction Sonde has two significant advantages for the measurement of refractive index. The first is the small size and light weight of the sonde which simplifies field operation. A second advantage is the high vertical resolution of data due to the use of fast time commutation of the sensors.

A 0.1-second switching rate is used to commutate each of the temperature, pressure and humidity sensors. A complete cycle is completed every 400 milliseconds. At a balloon ascent rate of 800 feet per minute, this gives a vertical resolution of 5.33 feet. In other words, the temperature, humidity, altitude and refractive index are sampled every 5.33 feet of ascent. This gives a very fine resolution to the analysis of refractive layers.

As an illustration of this resolution, refer to Figure 15. A weak inversion layer was located at 600 meters during the first flight. This layer can be detected by the slight inflection or bump in the N and M curves. It is difficult to see much of the character of the refractive index at this scale; therefore, the N and M values were replotted for the first 1000 meters of the flight as shown in Figure 31. This plot shows the refractive index at each of the contact points of the NWS Rawinsonde. Although this shows the refractive layer more clearly, it is still hard to see the fine structure.

A plot of the N and M values, measured with the Mini-Refraction Sonde for the first 1000 meters of flight, is shown in Figure 32. This plot shows the 2-meter altitude resolution of the MRS. The refractive layer can clearly be seen. It starts at 460 meters and ends at 770 meters. This demonstrates the value of the high data rate available from the time-commutated Mini-Refraction Sonde.

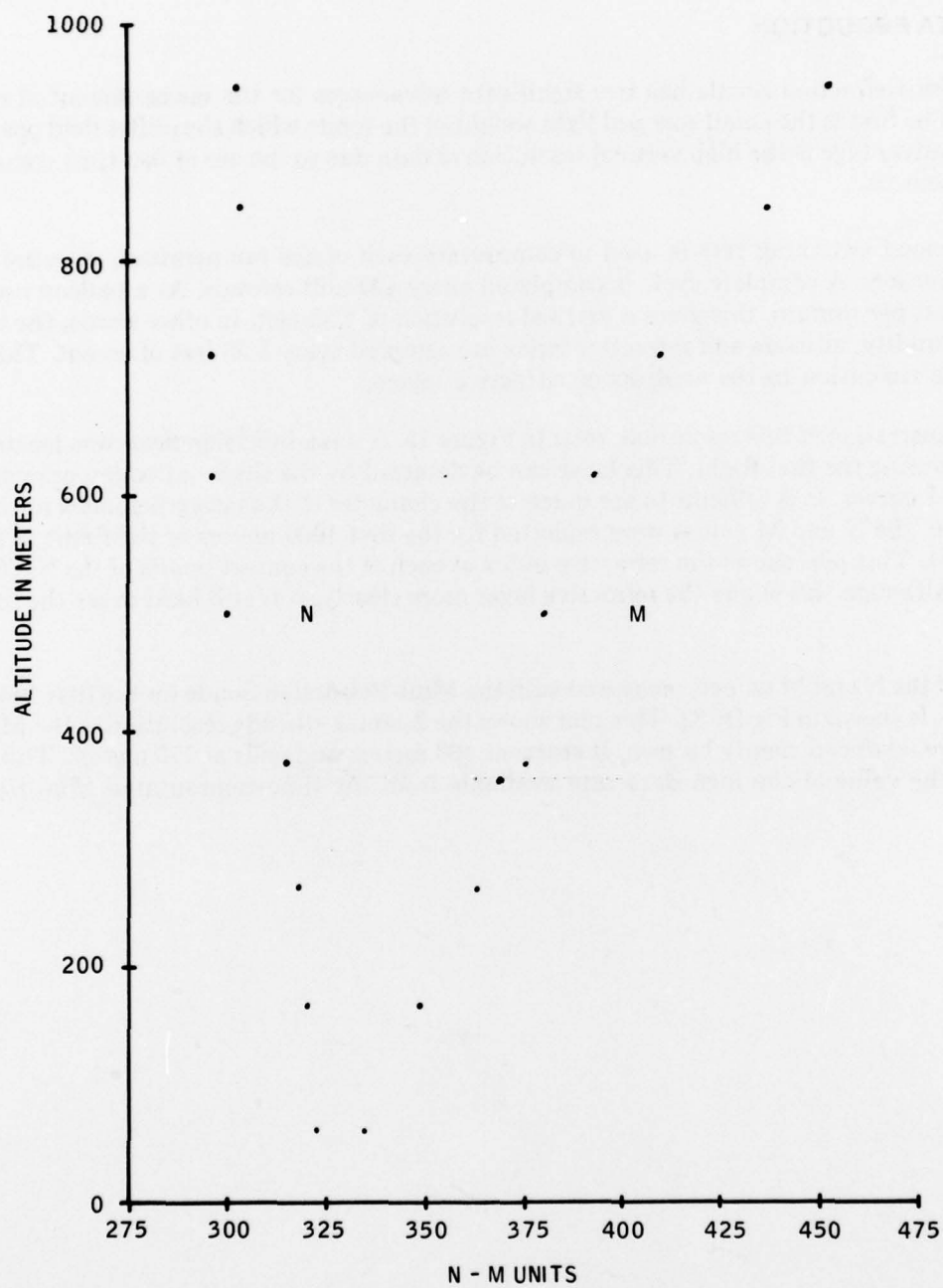


Figure 31. Plot of N and M versus Altitude for the First 1000 Meters of Flight Number 1 — Data Plotted at Switch Points Only

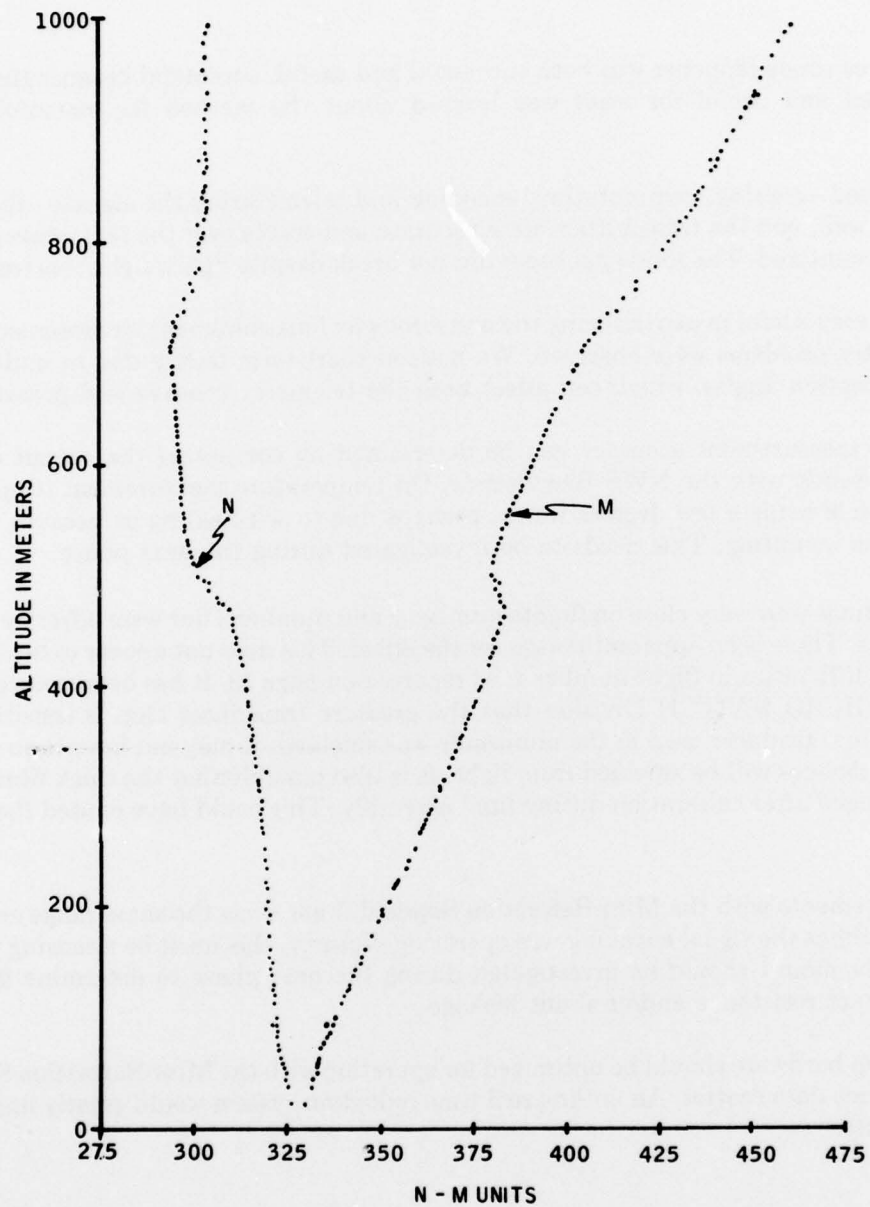


Figure 32. Plot of N and M versus Altitude for the First 1000 Meters of Flight Number 1 — Data Plotted for most of the Outputs of the Mini-Refracton Sonde at 2-1/2 Samples Per Second

IV. Conclusions

This series of three sonde launches was both successful and useful, successful because the total system functioned and useful for what was learned about the method for meteorological soundings.

All sondes operated—sensing, commutating, encoding and telemetering the signals—the batteries performed well, and the transmitters were accurate and stable over the temperature and voltage range encountered. The sonde packages did not break despite lightweight construction.

These tests were very useful in experiencing the meteorological measurement environment, and potential telemetry problems were observed. We noticed short term fading due to multipath fading at low reception angles, which can affect both the telemetry receiver and processor.

An indication of measurement accuracy can be determined by comparing the output of the Mini-Refraction Sonde with the NWS Rawinsonde. On temperature measurement it appears that the MRS sonde reads a few degrees warm, perhaps due to self-heating or because of the thermal lag of the mounting. This needs to be investigated during the next phase.

The pressure readings were very close on flights number 2 and number 3 but were offset by 5 mB on flight number 1. There is no apparent reason for the offset. This does not appear to be caused by the telemetry difficulties in flight number 1, as reported on page 13. It has been pointed out by Honeywell's MICRO SWITCH Division that the pressure transducer chip is sensitive to light. Although the transducer used in the minisonde was shielded, it may not have been light-tight. The future devices will be shielded from light. It is also possible that the thick film electronics were damaged after calibration during final assembly. This could have caused the calibration offset.

Humidity measurements with the Mini-Refraction Sonde did not show the same range as with the NWS Sonde. Since the signal encoding was operating properly, this must be a sensing problem. The hygistor mount should be investigated during the next phase to determine if it is causing high contact resistance and/or shunt leakage.

The data reduction hardware should be optimized for operating with the Mini-Refraction Sonde equipment to reduce data scatter. An on-line real time reduction system would greatly improve field measurements.

Appendix A Acknowledgements

We wish to thank the personnel of NASA for their guidance and assistance as well as the excellent facilities support at Wallops Island, Virginia. We also wish to acknowledge the following personnel from NADC for their capable assistance in the performance of these flight tests.

NASA

Bill Lord
Ray Atkins
Joe Paranzino

NADC

Ed Schmidt
Ralph Sellitsch